UCLA
UCLA Previously Published Works

Title

Ecosystem heterogeneity and diversity mitigate Amazon forest resilience to frequent extreme droughts

Permalink

https://escholarship.org/uc/item/4h16n3f5

Journal

New Phytologist, 219(3)

ISSN

0028-646X

Authors

Longo, Marcos
Knox, Ryan G
Levine, Naomi M
et al.

Publication Date

2018-08-01

DOI

10.1111/nph.15185

Peer reviewed

Ecosystem heterogeneity and diversity mitigate Amazon forest resilience to frequent extreme droughts

Marcos Longo[1,2] (iD)**, Ryan G. Knox**[3]**, Naomi M. Levine**[4]**, Luciana F. Alves**[5] (iD)**, Damien Bonal**[6]**, Plinio B. Camargo**[7]**, David R. Fitzjarrald**[8]**, Matthew N. Hayek**[1]**, Natalia Restrepo-Coupe**[9,10]**, Scott R. Saleska**[10]**, Rodrigo da Silva**[11]**, Scott C. Stark**[12]**, Raphael P. Tapajós**[11]**, Kenia T. Wiedemann**[1]**, Ke Zhang**[13]**, Steven C. Wofsy**[1] **and Paul R. Moorcroft**[1]

[1]Faculty of Arts and Sciences, Harvard University, Cambridge, MA 02138, USA; [2]Jet Propulsion Laboratory, California Institute of Technology, Pasadena, CA 91109, USA; [3]Lawrence Berkeley National Laboratory, Berkeley, CA 94720, USA; [4]University of Southern California, Los Angeles, CA 90007, USA; [5]Center for Tropical Research, Institute of the Environment and Sustainability, UCLA, Los Angeles, CA 90095, USA; [6]INRA, UMR EEF, 54280 Champenoux, France; [7]Centro de Energia Nuclear na Agricultura, Universidade de São Paulo, Piracicaba, SP 13416-000, Brazil; [8]University at Albany SUNY, Albany, NY 12222, USA; [9]Climate Change Cluster, University of Technology Sydney, Sydney, NSW 2007, Australia; [10]University of Arizona, Tucson, AZ 85721, USA; [11]Universidade Federal do Oeste do Pará, Santarém, PA 68040-255, USA; [12]Michigan State University, East Lansing, MI 48824, USA; [13]Hohai University, Nanjing, Jiangsu 210029, China

Author for correspondence:
Paul R. Moorcroft
Tel: +1 (617) 495 1621
Email: paul_moorcroft@harvard.edu

Summary

- The impact of increases in drought frequency on the Amazon forest's composition, structure and functioning remain uncertain. We used a process- and individual-based ecosystem model (ED2) to quantify the forest's vulnerability to increased drought recurrence.
- We generated meteorologically realistic, drier-than-observed rainfall scenarios for two Amazon forest sites, Paracou (wetter) and Tapajós (drier), to evaluate the impacts of more frequent droughts on forest biomass, structure and composition.
- The wet site was insensitive to the tested scenarios, whereas at the dry site biomass declined when average rainfall reduction exceeded 15%, due to high mortality of large-sized evergreen trees. Biomass losses persisted when year-long drought recurrence was shorter than 2–7 yr, depending upon soil texture and leaf phenology.
- From the site-level scenario results, we developed regionally applicable metrics to quantify the Amazon forest's climatological proximity to rainfall regimes likely to cause biomass loss > 20% in 50 yr according to ED2 predictions. Nearly 25% (1.8 million km²) of the Amazon forests could experience frequent droughts and biomass loss if mean annual rainfall or interannual variability changed by 2σ. At least 10% of the high-emission climate projections (CMIP5/RCP8.5 models) predict critically dry regimes over 25% of the Amazon forest area by 2100.

Introduction

The Amazon forest is the largest tropical rain forest in the world, storing *c.* 40% of the global biomass of tropical forests (Malhi *et al.*, 2006; Saatchi *et al.*, 2007, 2011). Research suggests that parts of the Amazon may be susceptible to biome shifts, biodiversity loss and depletion of carbon stores because of changes in climate and climate variability (e.g. Nobre & Borma, 2009; Marengo *et al.*, 2011; Davidson *et al.*, 2012; Anadón *et al.*, 2014; Duffy *et al.*, 2015; Boit *et al.*, 2016). Rainfall predictions for the region's 21st century climate are uncertain, but results from multiple model predictions indicate stronger and longer dry seasons, particularly in Southern and Eastern Amazonia (Malhi *et al.*, 2008; Fu *et al.*, 2013; IPCC, 2014; Boisier *et al.*, 2015), and increased recurrence of droughts (Duffy *et al.*, 2015), such as the widespread and intense Amazon droughts observed in 2005, 2010 and 2015–2016 (Marengo *et al.*, 2008; Phillips *et al.*, 2009;

Lewis *et al.*, 2011; Jiménez-Muñoz *et al.*, 2016; Erfanian *et al.*, 2017).

Terrestrial biosphere models suggest that CO_2 fertilization may reduce the die-back risk in the Amazon (e.g. Lapola *et al.*, 2009; Salazar & Nobre, 2010; Cox *et al.*, 2013; Huntingford *et al.*, 2013; Zhang *et al.*, 2015). However, the magnitude of the CO_2 fertilization effect is uncertain for two reasons. First, there is no direct observational or experimental evidence on the existence, magnitude and duration. Second, even less is known about changes in ecosystem water-use efficiency, photosynthetic capacity, and the effect of droughts on carbon uptake under elevated CO_2 (Rammig *et al.*, 2010), which may mean that the Amazon's vulnerability to droughts in warmer climates and high CO_2 may be over- or underestimated (Allen *et al.*, 2015; McDowell *et al.*, 2018). Additionally, future climate projections for the Amazon predicted by models participating in Phase 5 of the Climate Model Intercomparison Project (CMIP5) (Taylor *et al.*, 2012)

show great discrepancies because of the challenges to represent spatial distribution and seasonality in the Amazon (e.g. Joetzjer *et al.*, 2013; Yin *et al.*, 2013). Consequently, assessing the resilience, acclimation or susceptibility of the Amazon to changes in drought frequency is critical to understanding the current and future dynamics of the region's ecosystem.

Under high annual precipitation, above 2000 mm, and low-severity dry seasons (water deficit below 350 mm), water does not significantly limit productivity in tropical forests (Nemani *et al.*, 2003; Zelazowski *et al.*, 2011; Guan *et al.*, 2015; Ahlström *et al.*, 2017a). Eastern and Southern Amazon forests, which regularly experience multiple-month dry seasons (Davidson *et al.*, 2012), either show no seasonality or show increases in gross primary productivity (GPP) during the dry season (Hutyra *et al.*, 2007; Bonal *et al.*, 2008; Saleska *et al.*, 2009; Restrepo-Coupe *et al.*, 2013). However, results from natural droughts and drought experiments indicate that the Amazon forest is sensitive to changes in rainfall: mortality rates on forest plots increased after the 2005 and 2010 droughts (Phillips *et al.*, 2009; Feldpausch *et al.*, 2016), and net biomass accumulation, GPP and autotrophic respiration decreased during the 2010 drought (Doughty *et al.*, 2015; Feldpausch *et al.*, 2016). Furthermore, in two rain-exclusion experiments carried out in the Eastern Amazon, mortality – most likely caused by hydraulic failure – increased significantly after 3 yr of drought, particularly among larger trees (Nepstad *et al.*, 2007; da Costa *et al.*, 2010; Meir *et al.*, 2015; Rowland *et al.*, 2015). However, rain-out experiments only test the effects of a single change in soil moisture input, whereas real droughts have variable severity and also affect temperature, vapor pressure deficit, intercepted water and incoming radiation (Allen *et al.*, 2015; Bonal *et al.*, 2016).

Dynamic global vegetation models (DGVMs) have been employed to understand the Amazon forest's response to changing climate (e.g. Senna *et al.*, 2009; Galbraith *et al.*, 2010; Good *et al.*, 2013; Boulton *et al.*, 2017). However, most DGVM studies represent Amazon ecosystems as a single plant functional type (Moorcroft, 2003; Purves & Pacala, 2008; Evans, 2012). By contrast, observations suggest that forest responses to droughts emerge from responses of individual plant function and demographic performance (Bonal *et al.*, 2016), and there is evidence of significant differences in drought-induced mortality between genera, life form and size (Nepstad *et al.*, 2007; da Costa *et al.*, 2010; Esquivel-Muelbert *et al.*, 2017).

In this study, we investigate the resilience of different areas of the Amazon forest to changes in the region's rainfall regimes, with focus on the recurrence of extreme drought events using a process- and individual-based terrestrial biosphere model, the Ecosystem Demography Model version 2 (ED2; Medvigy *et al.*, 2009). ED2 has been shown to successfully represent the spatial variability of forest structure and dynamics, the timing of biomass loss due to droughts, and the forest's response to dry season length (Powell *et al.*, 2013; Zhang *et al.*, 2015; Levine *et al.*, 2016). ED2 simulations are used to explore the abiotic and biotic determinants of Amazon ecosystem responses to drought, examining the impacts of drought severity, soil texture and plant traits. In the first part of the analysis we investigate the predicted

ecosystem responses to changes in rainfall regime at a wetter tropical forest site in French Guiana (Paracou) and a drier tropical forest in Brazil (Tapajós) for which 40-yr-long time-series of rainfall measurements were available. In the second part, we draw upon this analysis to identify those areas of the Amazon that are most and least sensitive to changes in drought recurrence, by estimating how much the frequency distribution of annual rainfall would need to change before the ecosystem experiences significant tree mortality and biomass loss, and the likelihood that such changes will occur by the end of the 21st century.

Materials and Methods

Overview of study sites

In order to understand the relationship between drought occurrence and resulting changes in structure and composition, we examined predictions for two old-growth, evergreen broadleaf forest sites located at the wet and dry end-points of the precipitation gradient across the Amazon (Fig. 1). We selected these two focal sites because both areas had decade-long, high-frequency measurements of meteorological variables, and forest inventory measurements of tree growth and mortality rates (see Supporting Information Notes S1 for description of the site measurements). Long-term time series allowed us to generate realistic meteorological drivers that characterize their day-to-day variability, whose role in modulating the ecosystem dynamics has been demonstrated previously (Medvigy *et al.*, 2010).

The wet site is the Guyaflux tower (GYF) located at the Paracou Field Station, French Guiana (5°17′N; 52°55′W), a site with a closed-canopy forest with mean canopy height of 35 m (Bonal *et al.*, 2008). Annual rainfall at GYF averages 3050 mm, with a 4-month long dry season from August to November (Gourlet-Fleury *et al.*, 2004). Both deep, well-drained soils, and soils with impeding layers are found in the area (Epron *et al.*, 2006).

The dry site is in the Tapajós National Forest (TNF), Brazil (2°51′S; 54°58′W). This evergreen forest has a closed canopy
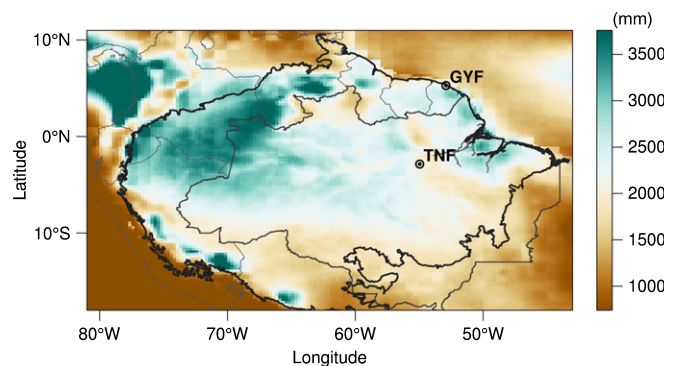

Fig. 1 Mean annual rainfall in tropical South America (1998–2015). Annual averages were obtained from the Tropical Rainfall Measurement Mission (TRMM), product 3B43 (Liu *et al.*, 2012). The thick black contour is the extent of the Amazon ecoregion, the thick gray contour is the extent of the Brazilian Legal Amazon and thin lines are the political boundaries. The locations of the two focal study sites (GYF, Guyaflux; TNF, Tapajós) are also shown.

with mean tree height of 40 m (Saleska *et al.*, 2003). Mean annual rainfall is 1900 mm, with a 5-month-long dry season from mid-July until mid-December (da Rocha *et al.*, 2009); rainfall shows high spatial variability depending on the distance to rivers and topography (Fitzjarrald *et al.*, 2008). Soils at TNF show no impeding layers until at least 12 m belowground (Nepstad *et al.*, 2007).

Ecosystem Demography Model, version 2

Like its predecessor, the Ecosystem Demography Model (ED) (Moorcroft *et al.*, 2001), in version 2 (ED2) the aboveground ecosystem is heterogeneous, characterized by a hierarchical structure that represents the horizontal and vertical heterogeneity of canopy structure and composition. The ecosystem within each area of interest (either a site, or a climatological grid cell) is represented using a set of size- and age-structured partial differential equations that represent the dynamics of a vertically and horizontally heterogeneous plant canopy comprising several different plant functional types (PFTs) (eqns 2.1–2.4 of Medvigy & Moorcroft, 2012). The most up-to-date model version (Knox, 2012; Longo, 2014) incorporates comprehensive biophysical and biogeochemical modules that solve the coupled energy, water and carbon budgets of the plants within the canopy at sub-daily scale and thus it accounts for important effects of day-to-day and within-day variability (Medvigy *et al.*, 2010). Although nutrient availability, particularly phosphorus (P), is also an important driver of tropical forest productivity (Santiago & Goldstein, 2016; Yang *et al.* 2016), this version of ED2 does not include process-based nitrogen (N) and P cycles. Detailed descriptions of the model formulation can be found in Medvigy *et al.* (2009), Knox (2012) and Longo (2014). A summary of the key aspects of the model for this study can be found in the Notes S2.

The ability of the ED2 model to characterize the long-term dynamics of Amazonian forests has been demonstrated previously (see Fig. S1; Notes S3; Powell *et al.*, 2013; Longo, 2014; Zhang *et al.*, 2015; Levine *et al.*, 2016). In addition, we present the most relevant model assessments based on eddy covariance fluxes (Fig. S2; Notes S3) and inventories from the study sites (Fig. S3; Notes S3). Importantly, the seasonal cycle of available water simulated by ED2 also showed good agreement with field measurements at both sites, although the model tends to overestimate available water during the wet season at TNF and all year at GYF (Fig. S2e,f; Notes S3).

Rainfall regime scenarios and simulation design

In order to describe the current rainfall regimes, we used historical rainfall data from conventional weather stations near the study sites that have reported daily rainfall since at least 1972: Cayenne (WMO-81405), located 80 km east of GYF, and Belterra (WMO-82246), located 25 km north of TNF. The probability distribution of annual rainfall (P, mm yr^{-1}) at each site was characterized by a skew-normal distribution

$p_{\mathrm{SN}}(P|\xi_{\mathrm{P}};\omega_{\mathrm{P}};\alpha_{\mathrm{P}})$ (Azzalini, 2005), whose location (ξ_{P}), scale (ω_{P}) and shape (α_{P}) parameters govern the mean (μ_{P}), standard deviation (σ_{P}) and skewness (γ_{P}) of the rainfall distribution (Fig. 2a; Notes S4). The historical rainfall data were used to develop a series of regimes with higher probability of extreme droughts. Each rainfall scenario is defined by a parameter S whose values (0, −0.2, −0.4, …, −1.6) indicate the change in the location parameter in units of the scale parameter (i.e. $\xi_{\mathrm{S}}=\xi_{\mathrm{P}}-S\cdot\omega_{\mathrm{P}}$). Because neither site showed any statistically significant autocorrelation in annual rainfall (Fig. S4), the rainfall regime scenarios were created by randomly sampling, with replacement, complete years taken from the historical datasets, using altered distribution functions $p_{\mathrm{SN}}(P|\xi_{\mathrm{S}};\omega_{\mathrm{P}};\alpha_{\mathrm{P}})$ (Fig. 2b). Simulations under scenario $S=0$ use parameters of the present-day rainfall regimes plus a simulation using the observed rainfall time series. Note that because we only sampled years from historical records, even the driest scenario at GYF was still rainier than the current climate at TNF (Fig. 2c,d). Nonetheless, through this procedure, the series of scenarios reflect a range of drier climate regimes while maintaining patterns of intra- and inter-annual variability rainfall within each scenario. Unless otherwise noted, simulations were carried out with atmospheric CO_2 concentration typical of the early 21st century (378 ppm).

In order to account for the range of effects of soil hydraulic properties on forest ecosystem response to drier regimes, and the uncertainties associated with the representation of hydraulic properties in ED2, we selected five soil texture classes that represent soils commonly found in the Amazon (Notes S5): clayey sand (CSa), sandy clay loam (SaCL), clay loam (CL), loamy sand (LSa) and clay (C).

Leaf phenological information was not available for all species occurring at the two sites, and thus simulations were conducted under the assumption that the plant community was either entirely evergreen or entirely drought-deciduous. Additional parameters and settings were kept constant for all simulations (Table S1). The combination of nine scenarios of changed rainfall patterns, 16 realizations of each scenario, five types of soil texture and two different leaf phenology configurations yielded 1440 simulations for each of the two sites. Each simulation was carried out for 60 yr, with the first forest inventory at each site (2004 at GYF and 1999 at TNF) being used to provide initial conditions for the model.

Drought and rainfall regime metrics

As will be shown in the Results section, the ED2 simulations for GYF and TNF exhibited a characteristic relationship between the recurrence of extreme droughts and biomass loss. From this relationship, we quantified, for different parts of the Amazon, the climatological proximity of the current rainfall regime to critically dry regimes that, according to ED2 predictions, would lead to sustained biomass losses, and the risk that such regime could be reached by year 2100.

We represented the relationship between the rate of biomass change (Δ_{AGB}) and the return interval of extreme droughts (τ_{D1})
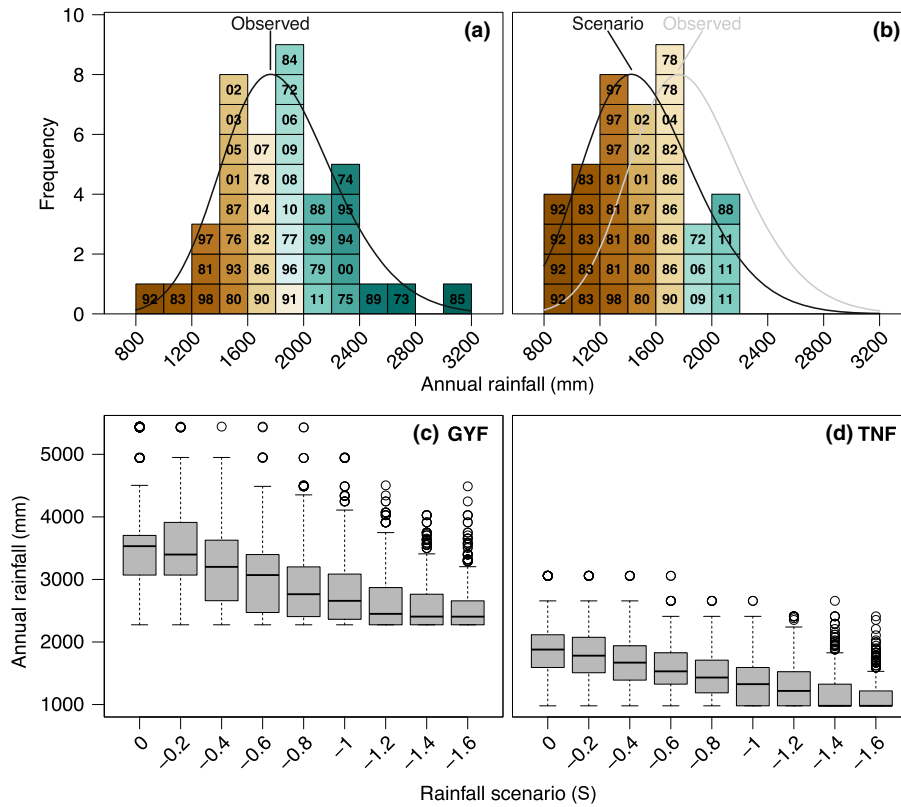
Fig. 2 Overview of the rainfall regime change scenarios. (a, b) Histogram of annual rainfall for site TNF for (a) the present-day rainfall regime and (b) one example of shifted rainfall regime scenario ($S = -0.6$). Black curves are the fitted skew-normal distribution of (a) original time series and (b) drier rainfall regime. Gray curve in (b) is the present-day rainfall regime, shown for reference. Numbered boxes are the last two digits of the (a) observed years and (b) observed years that were selected for the drier scenario, colored by total annual rainfall. (c, d) Box-and-whisker plot for annual rainfall for tested rainfall regimes. Distribution of annual rainfall for each tested scenario (parameter S that controls probability of selecting dry years) for sites (c) Guyaflux (GYF) and (d) Tapajós (TNF). Boxes span through the interquartile range, whiskers extend to 1.5 times the interquartile range, and horizontal lines inside boxes correspond to the median.

with hyperbolic curves:

$$(\Delta_{\mathrm{AGB}} - \Delta_0)\tau_{D1}^b = a \tag{1}$$

where (Δ_0; a; b) are coefficients that were fitted using a nonlinear robust estimator (Rousseeuw *et al.*, 2015). We defined extreme (year-long) droughts to be periods of water-deficit conditions that lasted at least 1 yr. The water-deficit calculations used actual evapotranspiration (ET) predicted by ED2, which accounts for the spatial and temporal variation in response to temperature, vapor pressure deficit, the canopy's leaf area index and the canopy response to levels of water stress.

We developed two metrics associated with one aspect of the forest's resilience, namely the precariousness (Folke *et al.*, 2004), defined in this manuscript as the climatological proximity of the current rainfall regime to critically dry rainfall regimes that would cause significant biomass loss. First, we characterized current regional rainfall regimes using a skew-normal distribution, based on precipitation data from six long-term, gridded datasets (Table 1; Fig. S5). We then used the fitted curves (Eqn 1) to define the ED2-based critical return interval of year-long droughts (τ_c). The threshold τ_c was set as the point of the fitted curve associated with 20% loss of aboveground biomass in 50 yr,

because at this point model simulations predict rapid decay in biomass with relatively small changes in the return interval of year-long droughts (see the Results section). Finally, we quantified precariousness either in terms of reduction of the mean annual rainfall (δ_μ), or increase of the standard deviation of the annual rainfall (δ_σ) relative to present-day rainfall regime (Fig. 3) that causes the return interval of year-long droughts to be τ_c (critically dry rainfall regime):

$$\delta_\mu = \min\left(0, \frac{\mu_P - \mu_c}{\sigma_P}\right), p_{\mathrm{SN}}(P \leq P_c | \mu_c, \sigma_P, \gamma_P) = \frac{1}{\tau_c} \tag{2}$$

$$\delta_\sigma = \min\left(0, \frac{\sigma_c - \sigma_P}{\sigma_P}\right), p_{\mathrm{SN}}(P \leq P_c | \mu_P, \sigma_c, \gamma_P) = \frac{1}{\tau_c} \tag{3}$$

(p_{SN}, the skew-normal probability distribution function given the mean (μ_P), standard deviation (σ_P) and skewness (γ_P) (Notes S3); μ_c and σ_c, critical statistics that make the mean return interval of year-long droughts equal to τ_c while keeping the other statistics the same). The precariousness metrics were calculated for each rainfall dataset and combined using a weighted average that accounts for their accuracy and time span (Notes S6; Figs S5, S6; Table S2). For both metrics, zero means that the current

drought recurrence is shorter than τ_c (high precariousness), whereas higher values indicate that the current rainfall regime is further away from the ED2-based critically dry regime (low precariousness).

In order to explore the risk of Amazonian forest's reaching the critically dry regime predicted by ED2 by the end of the 21st century, we obtained the output of 40 climate models of the Phase 5 of the Coupled Model Intercomparison Project (CMIP5, Taylor *et al.*, 2012). For each climate model, we selected one ensemble member, reprojected all models to a 1-degree grid, and used the last 40 yr of 21st century simulations under the RCP8.5 (high-emission) scenario (Table S3). Most CMIP5 models show significant precipitation biases relative to observations in the Amazon during the historical period (e.g. Joetzjer *et al.*, 2013); therefore, we applied a quantile mapping bias correction that preserves the relative changes in precipitation between the historical period and future scenarios (method QDM from Cannon *et al.*, 2015). We then fitted skew-normal distributions to their annual rainfall predictions for the late 21st century and computed the return interval of year-long droughts for each model *m*, and then obtained the fraction of models ($f_{RCP8.5}$) that predicted $\tau_m < \tau_c$ at each grid cell. Areas with higher fraction ($f_{RCP8.5}$) indicate higher agreement among climate predictions that the rainfall regime is likely to exceed the predicted threshold of critically dry regime by year 2100. The source code for the ED2 model, information on the input data and the rainfall regime scenario scripts are available in Notes S7.

Results

Site-level simulations

The simulated shifts in rainfall regimes resulted in markedly different ecosystem responses at GYF and TNF. At GYF, the mean aboveground biomass (AGB) differed by < 3% for all realizations under the different rainfall regimes, soil texture types and leaf phenology schemes (Fig. 4a,b). By contrast, at TNF, drier scenarios yielded considerable biomass loss (Fig. 4c,d). The point at which average AGB became significantly lower than the control scenarios varied depending on soil texture: for clayey soils, mean AGB decreased by > 15% at $S = -0.8$ (a 20% reduction in mean rainfall), whereas for sandy soils, mean AGB decreased by *c.* 5%, indicating that simulations with sandy soils showed greater

resistance to changes in AGB compared to those with clayey soils (Fig. 4c,d). Biomass losses also were influenced by canopy phenology: under similar rainfall regimes, losses were more significant in evergreen communities (Fig. 4c) than in drought-deciduous counterparts (Fig. 4d). The predicted response to drier rainfall regimes was not restricted to changes in biomass: evapotranspiration, an important aspect of ecosystem function, also showed changes that were similar to the results for AGB. At GYF the model predicted minor (< 2%) increases of evapotranspiration under drier regimes (Fig. S7a,b), whereas at TNF evapotranspiration decreased between 12% (loamy sand, drought deciduous; Fig. S7d) and 16% (clay, evergreen; Fig. S7c) at scenario $S = -1.6$ (39% less rainfall).

Forests affected by droughts recovered much of their original biomass and structure during periods with sufficient rainfall (e.g. Fig. S8), as long as the return interval of year-long droughts (τ_{D1}) did not drop below 1.5–7 yr (Fig. 5a,b). As a reference, the return interval of year-long droughts, estimated from the meteorological data (1972–2011), is near 20 yr at TNF and over 200 years at GYF.

From the fitted hyperbolic curves (Eqn 1; coefficients shown in Table 2), we defined the critical return intervals (τ_c) and critical rates of biomass change (Δ_c) to be the points on the fitted curve where the rate of aboveground biomass loss would be equivalent to 20% loss over a 50-yr period. This definition was chosen because it corresponds to the point at which aboveground biomass declines rapidly with further reduction in the return interval (Fig. 5). The critical return interval values (Table 2) were used to define the climatological proximity measures, δ_μ and δ_σ (Eqns 2, 3).

At GYF, the average basal area in the driest scenarios was 1–3% higher than the control for most size classes and plant functional types (PFTs) (Fig. 6a,b) due to sunnier conditions, and both growth and mortality rates remained similar for all scenarios (Figs S11a,b, S12a,b). By contrast, the forest structure for the driest scenarios at TNF differed substantially from the control: in the evergreen simulations (Fig. 6c), early-successional trees went extinct in most realizations under the $S = -1.4$ and $S = -1.6$ scenarios (35–39% reduction in mean rainfall, respectively). Extreme loss of early-successional trees was partially compensated for by the increased abundance of mid-successional individuals, whose basal area in the driest scenarios were higher by 165% in small and mid-size classes (DBH < 35 cm). Late successional trees

Table 1 Gridded rainfall datasets used to characterize present-day rainfall regimes

Dataset	Name	Resolution[a]	Period[b]	Reference
PGMF	Princeton University Global Meteorological Forcing	1.0	1969–2008	Sheffield *et al.* (2006)
UDel-3.01	University of Delaware	0.5	1969–2008	Matsuura & Willmott (2012)
GPCC-6.0	Global Precipitation Climatology Centre	1.0	1969–2008	Schneider *et al.* (2014)
PREC-L	NOAA's Precipitation Reconstruction over Land	1.0	1969–2008	Chen *et al.* (2002)
GPCP-2.2	Global Precipitation Climate Project	2.5	1979–2012	Huffman *et al.* (2009)
TRMM/3B43-7.0	NASA Tropical Rainfall Measurement Mission	0.25	1998–2012	Liu *et al.* (2012)

[a]Native resolution in degrees. All datasets were reprojected to 1° resolution grids.
[b]Time period was restricted to a maximum of 40 yr to be consistent with the site-level simulations (1969–2012). Because GPCC-2.2 and TRMM/3B43-7.0 had shorter time series, we used all available years until 2012.
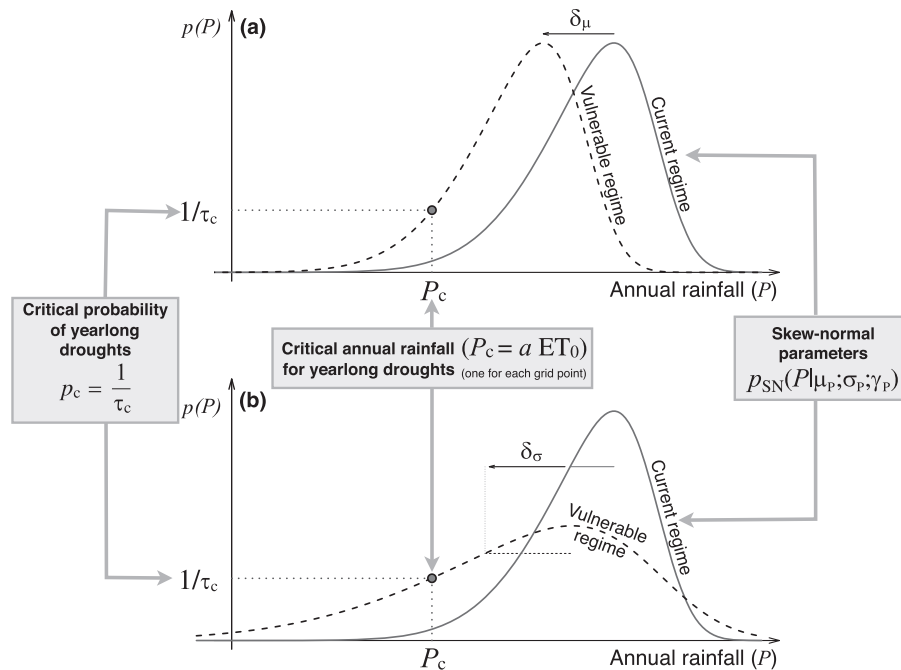
Fig. 3 Schematics of the method used in this study to quantify the Amazon forest proximity to critical rainfall regimes for each grid point. (a) Proximity caused by a shift in the mean rainfall regime (δ_μ); (b) proximity caused by a change in the inter-annual variability (δ_σ). The remaining symbols are defined as follows: p_{SN} (μ_P; σ_P; γ_P) is the skew-normal distribution of annual rainfall P and characterized by the mean (μ_P), SD (σ_P) and skewness (γ_P); τ_c is the critical return interval of year-long droughts; and P_c is the critical annual rainfall for year-long droughts and depends on the climatological evapotranspiration ET_0.

were lost in all size classes regardless of their leaf phenology (Fig. 6c,e).

At TNF, the impacts of drier climates also depended on tree size, with the largest trees experiencing losses, and smaller individuals becoming more abundant. The average basal area decreased with drier climates at TNF for all classes with DBH ≥ 10 cm, whereas subcanopy trees ($35 \leq DBH < 55$ cm) lost 87% of basal area between the wettest and the driest scenarios in the evergreen case (Fig. 6d), and *c.* 55% loss in the drought-deciduous case (Fig. 6f). Trees with DBH < 10 cm increased basal area by 35% for the evergreen case (Fig. 6d), although these trees remained little-affected (8% less basal area) in the drought-deciduous case (Fig. 6e). Changes in the forest structure resulted from general reduction of growth rates among larger trees (Fig. S11d,f) and the increase in environmentally determined mortality for all plant functional types and DBH classes as the climate became drier, with increases being more pronounced in the evergreen phenology case (Fig. S12c–f). The highest community-level mortality rates and lowest growth rates occurred when droughts lasted longer than 20–50 months (Fig. S13c,d,g,h).

At TNF, reductions in both leaf-level gross primary productivity (33% or 0.7 kgC m^{-2} yr^{-1}; Fig. S14a) and stomatal conductance (32% or 26 kg m^{-2} yr^{-1}; Fig. S14b) for large trees caused decreased growth and increased mortality. The response of large trees to drier climate was dominated by additional water stress, both below- and aboveground (Fig. S14c,d). By contrast, stomatal conductance and GPP for small trees increased as a result of the loss of large trees that allowed more light to reach the

understory (Fig. S14b,e). Higher productivity resulted in higher growth rates for small trees, which compensated for the increased mortality rates caused by higher drought frequency (Fig. S12c–f).

Regional drought vulnerability

The results from simulations for the focal sites indicate that the recurrence of year-long droughts is a strong predictor of biomass loss in tropical forests (Fig. 5). Because the tropical plant functional types in ED2 are not specifically developed for the study sites, and the driving equations of the model rely on general principles of ecosystem dynamics, we used this relationship between return interval and biomass to explore and quantify the vulnerability of different Amazon forest regions to changes in rainfall regimes, as explained in the Materials and Methods section and Fig. 3.

The climatological annual evapotranspiration ET_0 for the Amazon was calculated from a 40-yr regional potential vegetation simulation after the vegetation had reached equilibrium. The basin-wide average ET_0 (Fig. 7a) is 1160 mm yr^{-1}, a value which is close to the common assumption of 100 mm per month (e.g. Malhi *et al.*, 2009); ET_0 also was assessed and found to be consistent with both independent regional estimates and data from eddy covariance towers (Notes S3; Longo, 2014). Importantly, ET_0 varies across the region, with the highest values at the warmer regions at the forest-savanna transition, such as the arc from Tocantins (TO) to El Beni (B) and Eastern Roraima (RR), and the lowest values at the cooler regions such as the Andes slopes, and high cloud-cover areas such as the western Amazonas (AM) and the coast near the GYF site (Fig. 7a).
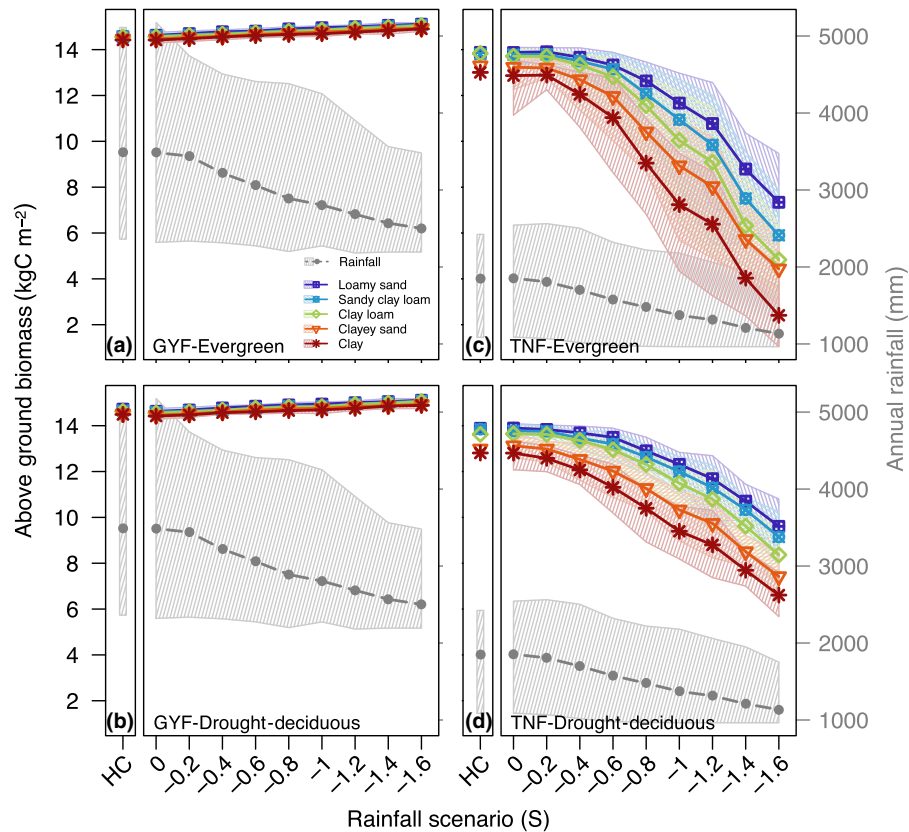
Fig. 4 Averaged aboveground biomass predicted by Ecosystem Demography Model version 2 (ED2 as a function of soil texture and rainfall scenario. (a) Guyaflux (GYF), evergreen; (b) GYF, drought-deciduous; (c) Tapajós (TNF), evergreen; and (d) TNF, drought-deciduous. Colored points and solid lines represent the mean of the 40-yr averages obtained for each realization, and the color-shaded region corresponds to the 2.5–97.5% quantile range of the 40-yr averages. HC corresponds to the simulation results when the model is driven by the observed historical rainfall regime (1972–2011); rainfall scenarios (S) correspond to the shift of the annual rainfall distribution relative to the current climate; gray points and gray solid lines represent the mean annual rainfall scenario and gray-shaded region represents the 2.5–97.5% quantile range of annual rainfall.
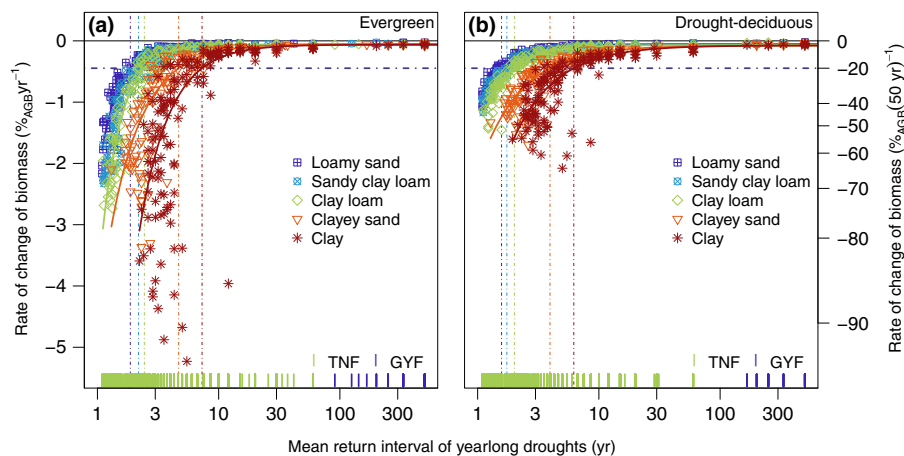

Fig. 5 Average rate of change in aboveground biomass as a function of the mean return interval of year-long droughts. Each point represents one simulation using (a) evergreen and (b) drought-deciduous phenology. Left axis shows the average rate of change in aboveground biomass (Δ_{AGB}) and right axis shows the equivalent Δ_{AGB} for a 50-yr period. Colors/symbols represent soil texture, and bottom lines represent the range of the mean return interval of year-long droughts (τ_{D1}) for each site. Thick color curves are the fitted curves for each soil texture, and dashed vertical lines are the critical return interval τ_c for each soil texture. Dashed horizontal line is the critical biomass loss (Δ_c).

In order to determine the dependence of critical annual precipitation (P_c) upon the climatological ET (ET$_0$; Fig. 3), we calculated the ratio between ET$_0$ and the total rainfall (calculated over

12-month periods) for every drought event on each grid cell that occurred between 1969 and 2008. The ratio approached one for droughts longer than 12 months (Fig. 7b), therefore we assumed

Table 2 Fitted models of aboveground change rate as a function of drought recurrence

Soil texture[a]	Phenology[b]	Δ_0[c, d, e]	a[c, d, f]	b[c, d, f]	τ_c[d]	R^2
LSa	EGN	−0.060 (0.007)*	−2.17 (0.05)	2.76 (0.08)	1.870 (0.020)	0.91
	DRD	−0.055 (0.005)***	−0.964 (0.020)	1.99 (0.07)	1.574 (0.012)	0.95
SaCL	EGN	0.065 (0.009)***	−2.98 (0.06)	2.64 (0.07)	2.18 (0.03)	0.91
	DRD	−0.065 (0.006)***	−1.068 (0.022)	1.85 (0.07)	1.745 (0.012)	0.96
CL	EGN	−0.068 (0.012)***	−3.97 (0.11)	2.64 (0.09)	2.44 (0.05)	0.90
	DRD	−0.069 (0.008)***	−1.363 (0.031)	1.84 (0.07)	2.010 (0.025)	0.90
CSa	EGN	−0.050 (0.030)*	−4.54 (0.31)	1.58 (0.10)	4.69 (0.30)	0.65
	DRD	−0.073 (0.017)***	−2.05 (0.10)	1.24 (0.07)	3.96 (0.14)	0.74
C	EGN	−0.06 (0.06)−	−12.3 (2.1)	1.74 (0.17)	7.3 (1.0)	0.40
	DRD	−0.08 (0.04)**	−3.6 (0.4)	1.25 (0.12)	6.2 (0.4)	0.59

[a]Soil texture classes are loamy sand (LSa), sandy clay loam (SaCL), clay loam (CL), clayey sand (CSa) and clay (C).
[b]Leaf phenology are evergreen (EGN) and drought deciduous (DRD).
[c]Coefficients were obtained for each soil texture and leaf phenology (one point for each simulation), using Eqn 1.
[d]Numbers in parentheses are the SE.
[e]−,*,**, and *** represent Δ_0 estimates that are statistically different from zero at the 0.1, 0.05, 0.01, and 0.001 confidence-levels, respectively.
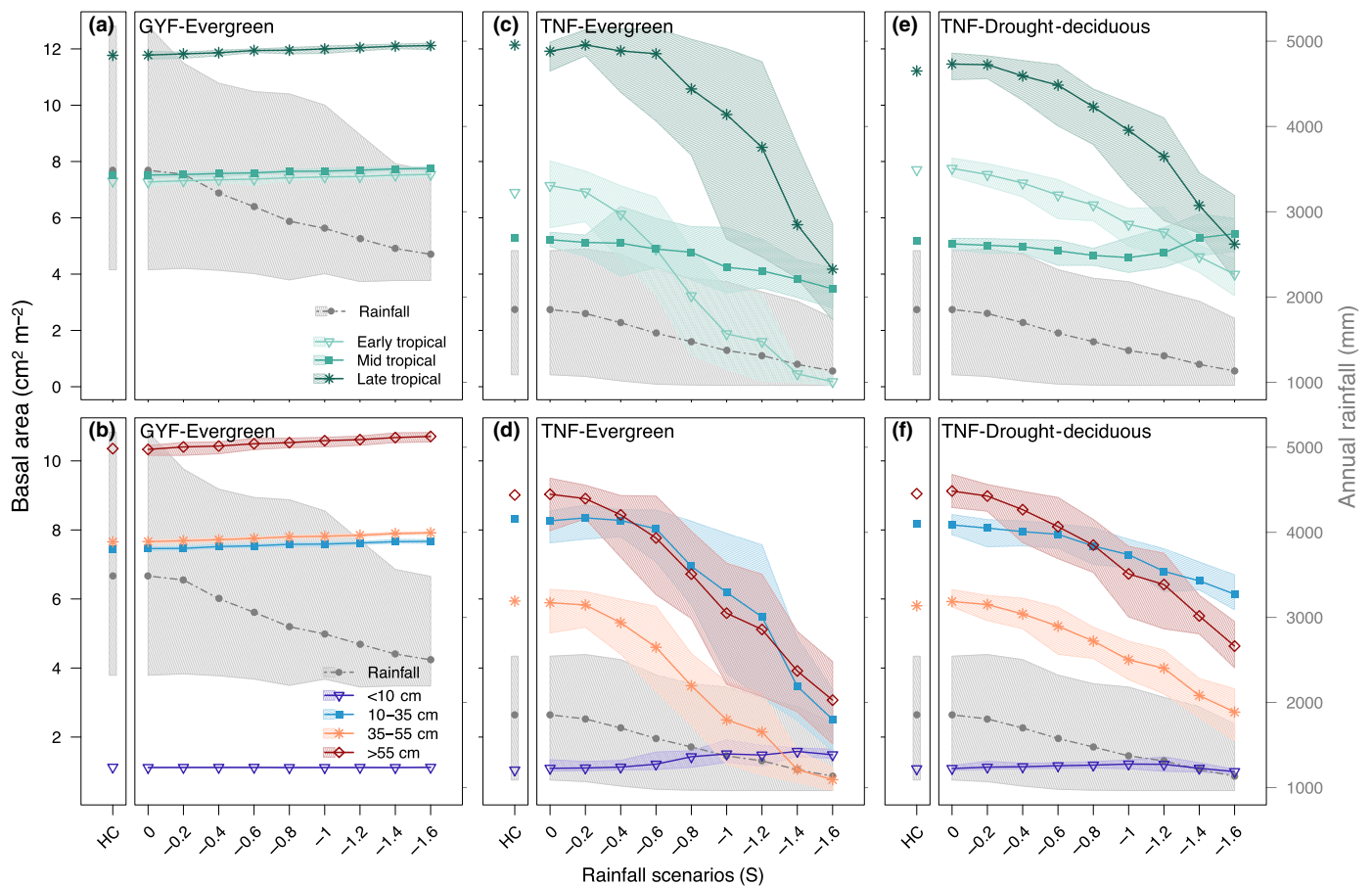[f]All estimates are statistically significant at the 0.001 confidence-level.

Fig. 6 Average size- and plant functional type (PFT)-structure of basal area as functions of rainfall scenarios. (a, b) Guyaflux (GYF) (evergreen), (c, d) Tapajós (TNF) (evergreen) and (e, f) TNF (drought-deciduous) for clayey sand simulations, disaggregated by (a, c, e) PFT and (b, d, f) size classes. Results for GYF (drought-deciduous) were nearly identical to the evergreen case and thus are not shown; results for other soil texture types are presented in Supporting Information Figs S9 and S10. Colored points and solid lines represent the mean of the 40-yr averages obtained for each realization, and the shaded region corresponds to the 2.5–97.5% quantile range of the 40-yr averages. HC corresponds to the simulation results when the model is driven by the observed historical rainfall regime (1972–2011); rainfall scenarios (S) correspond to the shift of the annual rainfall distribution relative to the current climate; gray points and gray dashed lines represent the mean annual rainfall scenario and the gray-shaded region represents the 2.5–97.5% quantile range of annual rainfall.
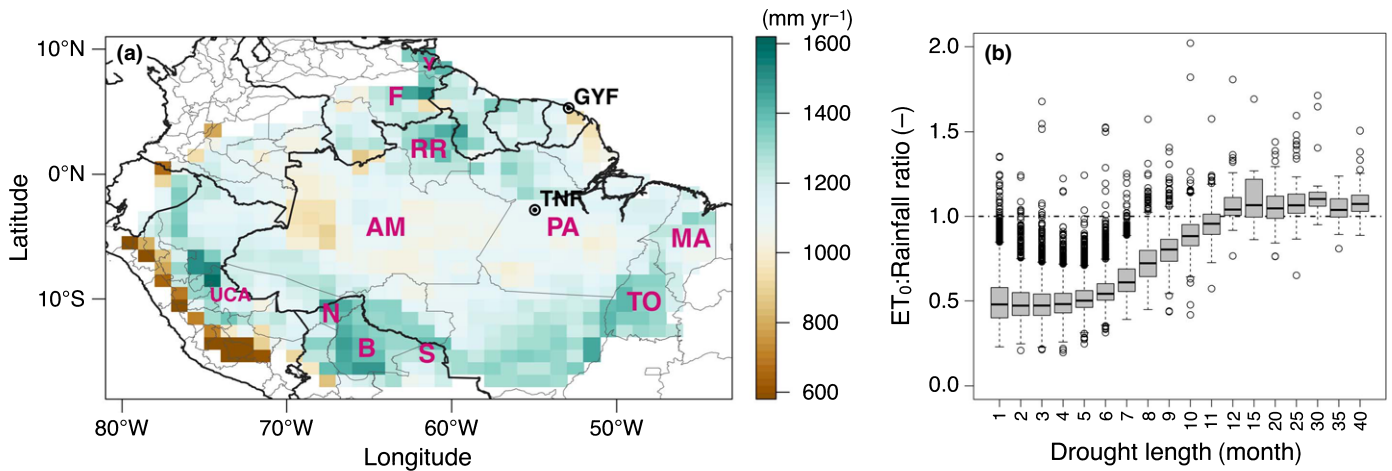
Fig. 7 Climatological evapotranspiration map and ratio between long-term evaporation and rainfall as a function of drought duration. (a) Average of climatological annual evapotranspiration (ET_0) simulated by ED2, using the last 40 yr of the 1500–2008 potential vegetation simulation. Brazilian States: Amazonas (AM), Roraima (RR), Pará (PA), Maranhão (MA), Tocantins (TO); Bolivian Departments: Santa Cruz (S), El Beni (B), Pando (N); Peruvian Regions: Ucayali (UCA); Venezuelan States: Bolívar (F), Delta Amacuro (Y). (b) Box plots of the ratio between long-term mean evapotranspiration and rainfall over the previous 12 months or entire drought duration for droughts that lasted longer than 12 months, as a function of drought length for all droughts reported in the Amazon grid; boxes span through the interquartile range, whiskers extend to 1.5 times the interquartile range, and horizontal lines inside boxes correspond to the median; the horizontal grid line corresponding to the ratio equal to 1 is shown for reference. Box plots separated by soil texture are shown in Supporting Information Fig. S15.

ET_0 to be a proxy for P_c. The critical return interval (τ_c) was obtained directly from Table 2, using the most similar soil texture for each grid cell and the values from drought deciduous phenology for a more conservative estimate. The annual rainfall distribution calculated for each gridded rainfall dataset is shown in Notes S6.

Modest changes in the current rainfall regime could bring large fractions of the Amazon to critically dry rainfall regimes according to ED2. Nearly 23% of the Amazon region (1.8 million km^2) would experience return intervals of year-long droughts below τ_c if the mean annual rainfall decreases, or if the standard deviation of annual rainfall increases by more than twice the current standard deviations (Table 3). Regions where the two precariousness metrics (Eqns 2, 3) indicated closeness to the threshold rainfall regime (i.e. near-zero δ_μ and δ_σ) were mainly nonforested regions, such as Delta Amacuro (Y), Bolívar (F), El Beni (B), Santa Cruz (S), Tocantins (TO), Maranhão (MA) and northern Roraima (RR). Within the Amazon, the shortest distances by shift in the mean annual rainfall (δ_μ) occurred in four regions: Northern Santa Cruz (S), Pando (N), Northern Ucayali (UCA) and a large band from central Roraima (RR) to Eastern Pará (PA), hereafter the Central-Eastern Amazon (Fig. 8a). The shortest distances associated with increased inter-annual variability in rainfall (δ_σ, Fig. 8b) could not be determined where the current mean rainfall was very high because the maximum probability of rainfall below P_c never reaches $1/\tau_c$, even if the standard deviation of annual rainfall approaches infinity. However, widespread δ_σ values below 2 at some of the driest areas in Central-Eastern Amazon, Northern Santa Cruz (S) and Pando (N) suggest that these regions could experience aboveground biomass loss through increased inter-annual variability, even if average annual rainfall remains similar. The results also indicate that a large area in

Southern Pará (dashed blue area in Fig. 8) would require major changes in rainfall to reach the critical rainfall, despite being close to the forest–savanna transition zone and not particularly wet. The high distance metrics result from a combination of lower ET associated with moderate altitudes (250–400 m above sea level) and cooler temperatures, and low rainfall inter-annual variability, particularly in the PGMF dataset.

The bias-corrected CMIP5 (RCP8.5) rainfall projections suggest that at least 90% ($f_{RCP8.5} < 10\%$) of the models agree that three quarters of the Amazon (5.9 million km^2) would not reach the ED2-derived definition of critically dry rainfall. By contrast, only 4% of the region (0.3 million km^2) had the majority of the models ($f_{RCP8.5} > 50\%$) predicting such critically dry conditions by the late 21st century (Table 3). For nearly one-fifth of the Amazon area (1.6 million km^2), between 10 and 50% of the models predicted that the return interval of year-long droughts would be shorter than τ_c (critically dry): these areas included Northern Santa Cruz and the Central-Eastern Amazon (Table 3; Fig. 8c). In addition, 15–30% of the models also indicate that extreme droughts would become critically recurrent in Suriname, even though δ_μ and δ_σ are not close to zero. Conversely, $f_{RCP8.5} < 5\%$ at Pando (N) despite the area showing low values for both distance metrics, because most models predicted increase in rainfall over that region.

Discussion

Site-level simulations

Impact of drought recurrence on biomass and ecosystem function In the present paper we explored the Amazon forest's vulnerability to changes in rainfall regime using a process-based

Table 3 Summary of the distance from critical rainfall regimes[a] and fraction of climate projections predicting critically dry regimes[a]

δ_μ[b,d] Range	10^3 km^2	%	δ_σ[c,d] Range	10^3 km^2	%	$f_{RCP8.5}$[e] Range	10^3 km^2	%
<0.0	96.4	1.2	<0.0	449	5.7	>70	170	2.2
0.0–1.0	763	9.7	0.0–1.0	752	9.5	50–70	170	2.2
1.0–2.0	973	12.3	1.0–2.0	648	8.2	30–50	364	4.6
2.0–3.0	1369	17.4	2.0–3.0	575	7.3	10–30	1246	15.8
≥3.0	4683	59.4	≥3.0	5462	69.3	≤10	5935	75.3

[a]Critically dry regimes were defined based on ED2 results (Table 2; Fig. 5).
[b]δ_μ is the reduction in mean annual rainfall to make the return interval of year-long droughts shorter than the critical return interval (τ_c).
[c]δ_σ is the increase in standard deviation of annual rainfall to make the return interval of year-long droughts shorter than τ_c.
[d]Both δ_μ and δ_σ were calculated by applying Eqns 2 and 3. The value presented is the weighted average of six rainfall datasets (Supporting Information Notes S4).
[e]$f_{RCP8.5}$ is the fraction of bias-corrected CMIP5 models predicting that the return interval of year-long droughts would be shorter than τ_c by the end of the 21st century.
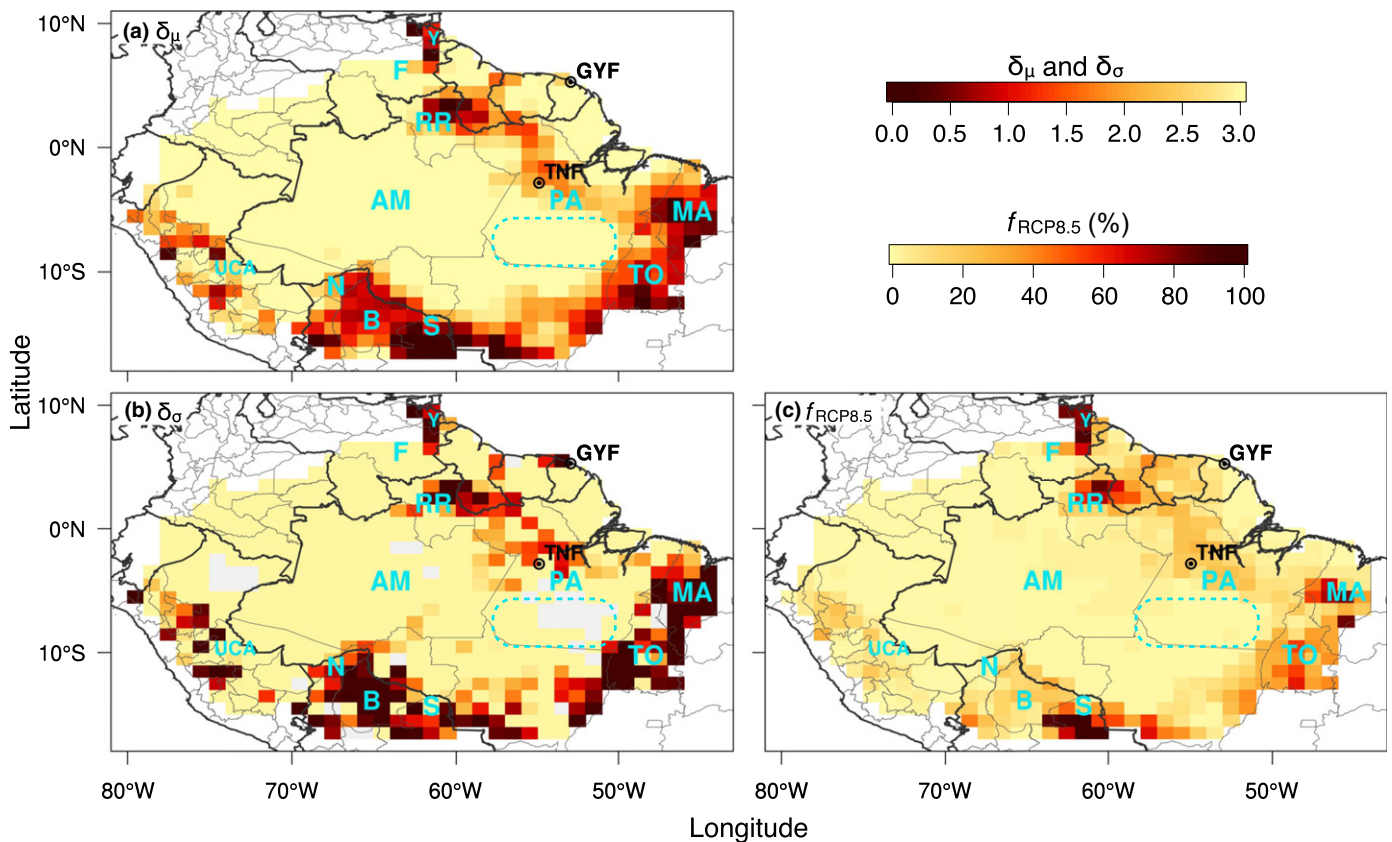

Fig. 8 Regional maps of distance from critical rainfall regimes and fraction of climate projections predicting critically dry regimes. Critically dry regimes are defined based on ED2 predictions of aboveground biomass loss when driven with early 21st century atmospheric CO_2 (see Table 2 and Fig. 5). (a) Reduction in mean annual rainfall (δ_μ) and (b) increase in standard deviation of annual rainfall (δ_σ) needed to make the return interval of year-long droughts shorter than the critical return interval (τ_c). Metrics δ_μ and δ_σ were calculated by applying Eqns 2 and 3 to six rainfall datasets and averaging them (Supporting Information Notes S6). Color intensities were truncated at 3 for clarity. Gray areas correspond to regions where no solution could be found (see main text). (c) Fraction of bias-corrected CMIP5 models predicting that the return interval of year-long droughts would be less than τ_c by the end of the 21st century under the high-emission (RCP8.5) scenario ($f_{RCP8.5}$). Brazilian States: Amazonas (AM), Roraima (RR), Pará (PA), Maranhão (MA), Tocantins (TO); Bolivian Departments: Santa Cruz (S), El Beni (B), Pando (N); Peruvian Regions: Ucayali (UCA); Venezuelan States: Bolívar (F), Delta Amacuro (Y). The rectangle in Southern Pará corresponds to the area with high δ_μ and δ_σ (low precariousness) described in the 'Regional drought vulnerability' section.

model (ED2, Ecosystem Demography Model version 2) in which the ecosystem's response to droughts reflect the ensemble response of individual plants of different sizes and functional types living in a variety of within-canopy micro-environments.

High-rainfall areas, such as Paracou, are predicted to be insensitive to moderately drier rainfall regimes (i.e. have low precariousness; Figs 4–6, S7): the typical wet season provides sufficient rainfall to recharge soils, and the drier scenarios simply reduce

water losses through runoff (Fig. S16), with minimal effects on water stress, and changes in biomass (Fig. 4), forest structure (Fig. 6) and evapotranspiration (Fig. S7). By contrast, drier forests, like the Tapajós, are less resilient (i.e. have high precariousness), and become severely water-limited, lose aboveground biomass and experience reductions in evapotranspiration under scenarios with $S = -0.6$ and drier (15% reduction in mean annual rainfall, to c. 1500 mm; Figs 4–6, S7). Our results suggest that historical El Niño-related droughts at the Tapajós (1991–1993, 1997–1998 and 2015–2016) were sufficiently strong to cause biomass loss, consistent with observational studies conducted in the early 2000s, which found that forests were recovering from a recent mortality event (Rice *et al.*, 2004; Pyle *et al.*, 2008), and a recent study that reported increased canopy turnover during the 2015–2016 drought (Leitold *et al.*, 2018). According to ED2 results, high-rainfall periods, akin to the typical wet season in Paracou, could reduce the impacts of strong droughts (Fig. S16). Over the past decades, extreme drought and extreme flood events have become increasingly common (e.g. Lewis *et al.*, 2011; Marengo *et al.*, 2012; Gloor *et al.*, 2013; Feldpausch *et al.*, 2016); however, extreme high-rainfall events have been mostly concentrated in the already wet northwestern areas (Gloor *et al.*, 2013), and thus have had limited impact on drought mitigation.

In drier forests such as Tapajós, canopy phenology is an important determinant of a forest's ecosystem sensitivity to droughts (Figs 4–6). The tropical leaf phenology scheme in ED2 assumes that evergreen trees utilize stored carbon to maintain their living tissues and maintain growth even during droughts, whereas drought-deciduous trees drop leaves and stop tissue growth when water-stressed (Notes S2). These different strategies are plausible hypotheses for how evergreen and drought-deciduous trees change their resource allocation during periods of water stress; however, Doughty *et al.* (2015) suggested that trees reduce maintenance of living tissues, while continuing to grow during droughts. Such a strategy would possibly result in responses to droughts that are intermediate between the existing evergreen and drought-deciduous formulations in ED2. Improved understanding of the environmental determinants of plant-level carbon allocation within Amazon forest trees is an important topic for future empirical studies (Comita & Engelbrecht, 2014; Wu *et al.*, 2016; Restrepo-Coupe *et al.*, 2017).

Impacts of soil hydraulic properties on the dynamics of biomass loss We found that, for a given rainfall regime, forests on sandier soils were more resilient (Figs 4, 5). This outcome results from clay particles being smaller and more compact; consequently, they bind water more strongly, bringing soils to the wilting point and water-stressed conditions more quickly (Longo, 2014; Levine *et al.*, 2016). This result may appear surprising because white sand forests in the Amazon have lower biomass and lower biodiversity, and white sand plant communities often show drought adaptations (Anderson, 1981; Jirka *et al.*, 2007; Saatchi *et al.*, 2011). However, in our simulations, soil texture only affected hydraulic parameters; in reality, higher sand content is usually associated also with lower nutrient availability,

shallower soils, and toxic aluminum concentrations (Laurance *et al.*, 1999; Fine *et al.*, 2006; Jiménez *et al.*, 2009). Moreover, the soil hydraulic parameterization used in ED2 is based on Cosby *et al.* (1984), which tends to overestimate the compactness of soils in the Amazon (Marthews *et al.*, 2014), and are not suitable for representing clay-rich soils. Although we restricted simulations to a maximum of 60% clay to conform with the range of data used by Cosby *et al.* (1984), the current parameterization does not account for diversity in soil organic carbon content and pore-size distributions. Nevertheless, our results imply that differences in soil hydraulic properties will mediate the Amazon ecosystem responses to changing rainfall regimes. As noted by Levine *et al.* (2016), it is critical to improve the mechanistic understanding of drought responses in different soil types, with modeling and field-based research to quantify the relative importance of soil hydraulic properties, soil nutrient content and drainage characteristics to the forest dynamics under future climate conditions.

Impacts of climate variability on change of forest structure and composition Our results indicate that large trees were more severely impacted by extreme droughts (Fig. 6d,f), in agreement with both experimental rain-out studies (Nepstad *et al.*, 2007; da Costa *et al.*, 2010) and pan-tropical observational studies (Phillips *et al.*, 2010). The simulated loss of canopy trees occurred because these trees are not light-limited, therefore additional light absorption did not increase productivity; instead, it caused higher respiration rates due to warmer leaves, and increased leaf vapor pressure deficit (LVPD). Conversely, the upper canopy losses improved light availability at the understory, causing small trees to proliferate (Figs 6, S5). It is important to point out that the simulated drought-driven mortality is entirely dependent on carbon balance. Additional mechanisms such as fire (Brando *et al.*, 2014) and hydraulic failure (Rowland *et al.*, 2015) could increase mortality at shorter time scales than carbon starvation only, and thus make forests even more susceptible to recurrent droughts.

Ecosystem transpiration rates affected competition for water between small and large individuals, leading to significant fluctuations of carbon balance during drought events (Fig. S17a). When deep soil layers, accessible only to tall trees, were already dry after long droughts (e.g. near simulation years 37–41 in Fig. S17b), having deep roots became less advantageous because the limited water supply is extracted from upper layers (accessible to all individuals) and transpired before it reaches deeper layers. In such situations, limited water supply strongly affects tall trees, because they demand more water, and experience higher temperatures and higher LVPD (Markewitz *et al.*, 2010; Ivanov *et al.*, 2012). The resulting water limitation, combined with higher carbon demand, significantly reduces the carbon balance among larger trees (Fig. S17a), which increases mortality and reduces growth (Fig. S13).

Differential responses within the canopy to the drier climate at Tapajós also depended on plant functional type composition (Fig. 6c,e). Water stress reduced productivity and severely impacted early successional trees because of their higher turnover

rates of leaves and fine roots (Reich *et al.*, 1997). By contrast, mid-successional trees with lower maintenance costs benefitted from the decline in early-successional trees. More generally, these results illustrate how Amazon forest canopies may respond to drier climates through changes in their size structure and plant functional type composition. This ability to reorganize canopy structure and composition in response to changes in precipitation regimes can increase the ecosystem adaptability, resulting in more gradual responses to climate changes than what would be obtained with 'big-leaf' representations of the ecosystem (see also Levine *et al.*, 2016; Sakschewski *et al.*, 2016).

Regional patterns of vulnerability

The predicted responses of the Amazon forests to drier rainfall regimes show significant biomass loss once the return interval of year-long droughts is < 2–7 yr (Fig. 5). The modeled critical return interval marginally overlaps with previous estimates and with typical drought recovery time in the Amazon (Hutyra *et al.*, 2005; Schwalm *et al.*, 2017), but also suggests that some forests could be even more vulnerable depending on biotic and abiotic controls, such as leaf phenology and soil hydraulic properties (Fig. 5). The ED2 simulations suggest that when the interval between droughts is too short, forest productivity during non-drought periods is insufficient to adequately recover the drought-driven biomass losses (Fig. S8). Similar to Feldpausch *et al.* (2016), we found that time since last severe drought explained < 3% of the variance in simulated net biomass change and productivity (Fig. S18), highlighting that simulated biomass losses do not result from the cumulative effects of extreme droughts on demographic rates.

A direct, regional evaluation of the Amazon response to different rainfall regimes at 1° resolution and using the same methodology used for the study sites was not computationally feasible, as it would require over 900 000 simulations. However, the ED2 model formulation used in this study has regional applicability (see also Zhang *et al.*, 2015; Levine *et al.*, 2016), making it possible to extrapolate the Paracou and Tapajós findings to whole Amazon biome scale, and thus to infer the regional risk of aboveground biomass (AGB) loss and accompanying changes of forest structure and composition due to changes in the rainfall.

Using the ED2-derived definition of critically dry regimes, substantial portions of the Central-Eastern Amazon are predicted to experience frequent extreme droughts and resulting biomass losses with either modest reductions in the mean rainfall or minor increases in the inter-annual variability (Fig. 8a,b). This region has been previously reported as vulnerable (e.g. Hutyra *et al.*, 2005; Hirota *et al.*, 2011; Anadón *et al.*, 2014), and 15–30% of the bias-corrected CMIP5–RCP8.5 models indicate that the region could reach the critically dry regime threshold by 2100 (Fig. 8c; see also Duffy *et al.*, 2015). Areas in Southwestern Amazon – Santa Cruz and Pando (Bolivia) and Ucayali (Peru) – are likewise near the critically dry rainfall regime, and have shown drying trends (Fu *et al.*, 2013; Gloor *et al.*, 2015), although most bias-corrected CMIP5-RCP8.5 projections suggest that the Pando would become wetter (Fig. 8c).

By contrast, Amazon areas along the Atlantic coast and in the Western region would require dramatic changes in their rainfall regimes before reaching the critically dry threshold (Fig. 8a,b). Nonetheless, 15–30% of the CMIP5 model projections indicate that Suriname could experience such dramatic change in rainfall (Fig. 8c). Interestingly, our analysis also indicates that forests in Southern Pará, Brazil (dashed area in Fig. 8a,b) are likely to be far from the critically dry threshold, despite their relatively low annual rainfall and being close to the forest–savanna transition zone. The higher resilience (low precariousness) of these regions arises from a combination of low inter-annual rainfall variability and lower evapotranspiration rates arising from the higher elevation and associated lower temperatures.

One limitation of our analysis is that it does not account for regional variation in traits: plants in drier parts of the Amazon may be more adapted and less vulnerable to droughts (Esquivel-Muelbert *et al.*, 2017). However, in case changes in the rainfall regime are rapid, their adaptation may be limited and insufficient to prevent major changes in carbon stocks and forest structure and composition (Allen *et al.*, 2015).

It is important to note that the model predictions that parts of the Amazon could reach critically dry regimes (Fig. 8) are contingent on the accuracy of the rainfall datasets and other climatic variables (temperature, radiation, humidity) used in the model simulations and subsequent analyses. Also, the coarse resolution (25–250 km) of the datasets means that local-scale topography and distance from large rivers, both known to affect the distribution of total annual rainfall (Fitzjarrald *et al.*, 2008), cannot be fully characterized. Moreover, in many of the areas identified above as either vulnerable or resilient, limited in-situ ecological and long-term meteorological observations are available (Fig. S6); measurements in these areas should be prioritized in future studies.

Impacts of elevated CO_2 on forest response to drier regimes

The forest responses predicted by ED2 emerged as a consequence of declining water availability. However, increasing atmospheric CO_2 also is likely to change the future functioning of forests (Rammig *et al.*, 2010; Cox *et al.*, 2013; Huntingford *et al.*, 2013; Zhang *et al.*, 2015). To explore the interactions between atmospheric CO_2 and rainfall regime, we performed 2880 additional simulations for the two study sites with the same characteristics described in the Methods section, with the exception of elevated atmospheric CO_2 concentrations (758 ppm), corresponding to the 2060–2099 average from CMIP5-RCP8.5 scenario (Meinshausen *et al.*, 2011).

Elevated-CO_2 simulations showed substantial biomass accumulation at both sites (5–60% compared to present-day biomass, Fig. 9), consistent with previous modeling studies that found that elevated CO_2 could offset deleterious effects of drier climate due to increased water-use efficiency (Cox *et al.*, 2013; Huntingford *et al.*, 2013; Farrior *et al.*, 2015; Zhang *et al.*, 2015). Nonetheless, the driest scenarios at Tapajós National Forest (TNF) ($S = -1.6$, or 39% reduction of mean annual rainfall) showed 10–38%

depletion in AGB when compared to present-day rainfall regimes ($S = 0$) and elevated CO_2 (Fig. 9c,d), as a consequence of increased water stress. Moreover, extreme drought recurrence ($\tau_{D1} < 3$ yr) reduced the rate of biomass accumulation by over 30% in 50 yr, relative to the elevated-CO_2, present-day rainfall regime (Fig. S19).

At the leaf level, high CO_2 increases photosynthetic activity through reduction of photorespiration, and reduces stomatal conductance and thus leaf-level water demand (Cernusak *et al.*, 2013). At the stand level, water demand also depends on changes in leaf area, which could compensate the higher water-use efficiency at leaf level (Würth *et al.*, 1998). In ED2 and under no water limitation, increased water-use efficiency was the dominant effect, reducing evapotranspiration by 8–10% in Guyaflux tower (GYF) (e.g. Fig. S20a,b). Conversely, evapotranspiration became similar to nonelevated CO_2 for the driest scenarios and clayey soils in TNF, indicating severe water limitation (Fig. S20c,d).

Although elevated-CO_2 simulations suggested a strong response of the forest and significant biomass accumulation (5–60% compared to present-day biomass), they likely overestimate the CO_2 fertilization effect. Previous model comparison studies showed that ED2 response to elevated CO_2 is strong

compared to other dynamic global vegetation models (Zhang *et al.*, 2015; Castanho *et al.*, 2016). Moreover, ED2 does not account for nutrient limitation such as phosphorous on photosynthesis in tropical forests (Santiago & Goldstein, 2016; Yang *et al.*, 2016). Furthermore, some studies suggest that carbon sinks by tropical forests are not becoming stronger carbon sinks as CO_2 increases (Clark *et al.*, 2013; Brienen *et al.*, 2015) and warmer temperatures may exacerbate the impacts of low rainfall during severe droughts (Allen *et al.*, 2015). The complex mechanisms that drive tropical forest dynamics under CO_2-rich, warmer, drier and nutrient-limited environments are still poorly understood, and efforts such as implementing a Free Air CO_2 Enrichment (FACE) experiment in the Amazon (Norby *et al.*, 2016) could provide much-needed data and significantly contribute to reduce uncertainties.

Concluding remarks and research priorities

Our analysis of regional ecosystem distance from critical rainfall regime presented here moves beyond prior studies (e.g. Hutyra *et al.*, 2005; Lapola *et al.*, 2009; Salazar & Nobre, 2010; Hirota *et al.*, 2011; Cox *et al.*, 2013) in three important respects. The
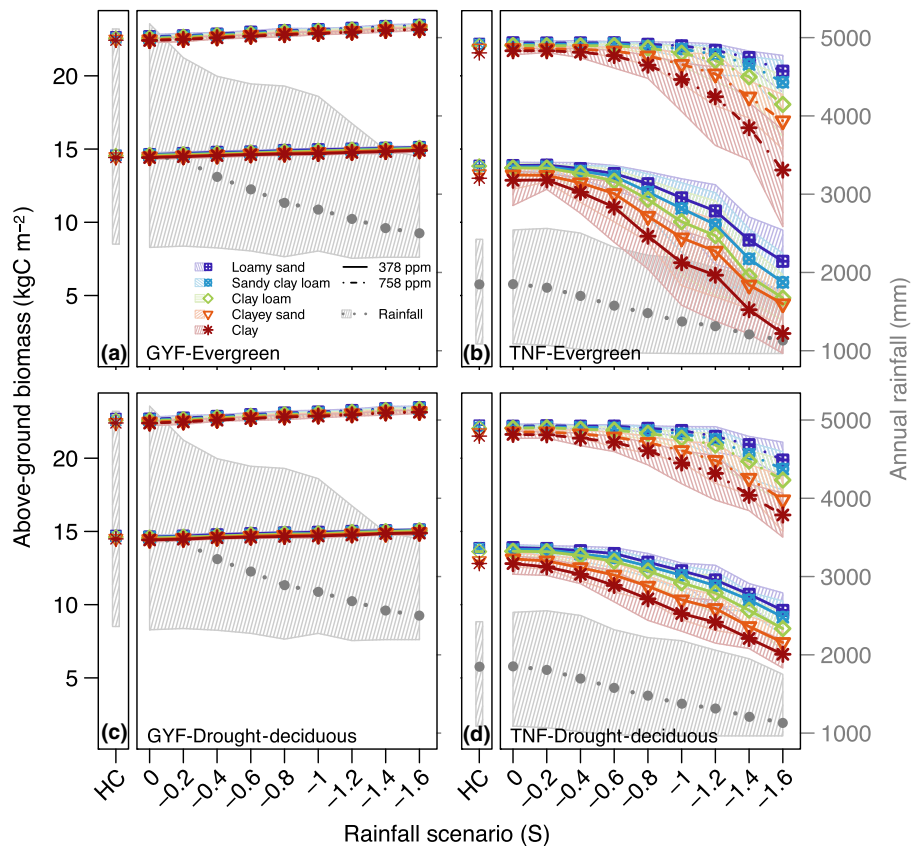

Fig. 9 Response of aboveground biomass predicted by ED2 under early and late 21st century atmospheric CO_2. (a) Guyaflux (GYF), evergreen; (b) GYF, drought-deciduous; (c) Tapajós (TNF), evergreen; and (d) TNF, drought-deciduous. Solid lines represent response using early 21st century atmospheric CO_2 (378 ppm), and dashed lines correspond to results under late 21st century atmospheric CO_2 under the high-emission scenario (758 ppm). Points represent the mean of the 40-yr averages obtained for each realization, and the shaded region corresponds to the 2.5–97.5% quantile range of the 40-yr averages. HC corresponds to the simulation results when the model is driven by the observed historical rainfall regime (1972–2011); rainfall scenarios (S) correspond to the shift of the annual rainfall distribution relative to the current climate; gray points and gray dotted lines represent the mean annual rainfall scenario and the gray-shaded region represents the 2.5–97.5% quantile range of annual rainfall.

analysis incorporates the effects arising from spatial variation in climate regimes and soil texture and differences in historical patterns of inter- and intra-annual variability that are key determinants of ecological dynamics (Zimmermann *et al.*, 2009; Reyer *et al.*, 2013). The predicted responses combine the ecological effects of size structure and competition for limiting resources between individuals of different plant functional types that affect ecosystem resilience (Levine *et al.*, 2016). We estimated forest vulnerability to drought based on continuous ecological variables such as community composition and biomass loss, as opposed to categorical distribution of biomes.

Additional mechanisms not included in our study are likely to contribute to the community response to changing and novel climates, and should be further investigated. First, there are still large uncertainties on many ecosystem parameters represented in the model (e.g. Fisher *et al.*, 2010). Also, leaf and stem hydraulic traits that drive drought tolerance (Maréchaux *et al.*, 2015; Rowland *et al.*, 2015; Powell *et al.*, 2017) were not directly incorporated in this version of ED2. A mechanistic plant hydraulics model has been recently implemented in ED2 (Xu *et al.*, 2016) and improved the ecosystem dynamics representation in Central America, although it has not been evaluated for the Amazon and does not represent hydraulic failure mortality. Additionally, drought-related mortality can result from other mechanisms, such as desiccation, reduced pest defense mechanisms and fires (van der Molen *et al.*, 2011; Brando *et al.*, 2014; McDowell *et al.*, 2018), which may further reduce the forest resistance to droughts. Also, the model results could only be evaluated against historical and present-day CO_2 concentrations (Notes S3), such that high-CO_2 simulations are unconstrained by observations; to answer the question of whether or not CO_2 fertilization will offset water limitation, the larger uncertainty of increasing CO_2, including the interactions between CO_2 fertilization and nutrient limitation, must first be addressed. Furthermore, changes in climate and in the plant community dynamics are highly interactive. Representing these interactions in Earth System Models requires ecosystem models that go beyond overly aggregated ('big-leaf') approaches. Previous multi-year studies have successfully integrated ED2 with regional atmospheric models at regional scales (e.g. Knox *et al.*, 2015; Swann *et al.*, 2015), and expanding the integration to the global scale is feasible, although it will also require reducing biases in climate projections (Ahlström *et al.*, 2017b).

In summary, our results highlight the importance of including ecosystem structure and composition in model predictions of future climate. For example, the loss of large resource-demanding, drought-intolerant trees in the most extreme drought scenarios also increased the light availability and thus reduced the impact of droughts on the understory. Representing changes in microenvironments experienced by individuals in an ecosystem is fundamental to understand the ecosystem dynamics under drought conditions, although it is fundamental to constrain and improve how plants with varying size and different life strategies access and compete for limiting resources such as water and light (Fisher *et al.*, 2018). Also, even though it is limited to one aspect of climate change and one ecosystem, our study shows that changes in

the interannual variability such as the frequency of extreme events, are likely to drive the fate of ecosystems as the climate changes.

Author contributions

M.L., S.C.W. and P.R.M. designed the research; M.L., R.G.K., N.M.L. and K.Z. developed the model; M.L. carried out the model simulations and analysis; L.F.A., D.B., P.B.C., D.R.F., M.N.H., N.R-C., S.R.S., R.d.S., S.C.S., R.P.T., K.T.W. and S.C.W. collected and pre-processed the meteorological and forest inventory data; and M.L., R.G.K., N.M.L., L.F.A., D.B., D.R.F., M.N.H., N.R-C., S.C.S., K.Z., S.C.W. and P.R.M. wrote the manuscript.

ORCID

Marcos Longo (iD) http://orcid.org/0000-0001-5062-6245
Luciana F. Alves (iD) http://orcid.org/0000-0002-8944-1851

References

Ahlström A, Canadell JG, Schurgers G, Wu M, Berry JA, Guan K, Jackson RB. 2017a. Hydrologic resilience and Amazon productivity. *Nature Communications* 8: 387.

Ahlström A, Schurgers G, Smith B. 2017b. The large influence of climate model bias on terrestrial carbon cycle simulations. *Environmental Research Letters* 12: 014004.

Allen CD, Breshears DD, McDowell NG. 2015. On underestimation of global vulnerability to tree mortality and forest die-off from hotter drought in the Anthropocene. *Ecosphere* 6: art129.

Anadón JD, Sala OE, Maestre FT. 2014. Climate change will increase savannas at the expense of forests and treeless vegetation in tropical and subtropical Americas. *Journal of Ecology* 102: 1363–1373.

Anderson AB. 1981. White-sand vegetation of Brazilian Amazonia. *Biotropica* 13: 199–210.

Azzalini A. 2005. The skew-normal distribution and related multivariate families. *Scandinavian Journal of Statistics* 32: 159–188.

Boisier JP, Ciais P, Ducharne A, Guimberteau M. 2015. Projected strengthening of Amazonian dry season by constrained climate model simulations. *Nature Climate Change* 5: 656–660.

Boit A, Sakschewski B, Boysen L, Cano-Crespo A, Clement J, Garcia-Alaniz N, Kok K, Kolb M, Langerwisch F, Rammig A et al. 2016. Large-scale impact of climate change vs. land-use change on future biome shifts in Latin America. *Global Change Biology* 22: 3689–3701.

Bonal D, Bosc A, Ponton S, Goret JY, Burban B, Gross P, Bonnefond JM, Elbers J, Longdoz B, Epron D et al. 2008. Impact of severe dry season on net ecosystem exchange in the Neotropical rainforest of French Guiana. *Global Change Biology* 14: 1917–1933.

Bonal D, Burban B, Stahl C, Wagner F, Hérault B. 2016. The response of tropical rainforests to drought—lessons from recent research and future prospects. *Annals of Forest Science* 73: 27–44.

Boulton CA, Booth BBB, Good P. 2017. Exploring uncertainty of Amazon dieback in a perturbed parameter Earth system ensemble. *Global Change Biology* 23: 5032–5044.

Brando PM, Balch JK, Nepstad DC, Morton DC, Putz FE, Coe MT, Silvério D, Macedo MN, Davidson EA, Nóbrega CC et al. 2014. Abrupt increases in Amazonian tree mortality due to drought–fire interactions. *Proceedings of the National Academy of Sciences, USA* 111: 6347–6352.

Brienen RJW, Phillips OL, Feldpausch TR, Gloor E, Baker TR, Lloyd J, Lopez-Gonzalez G, Monteagudo-Mendoza A, Malhi Y, Lewis SL et al. 2015. Long-term decline of the Amazon carbon sink. *Nature* 519: 344–348.

Cannon AJ, Sobie SR, Murdock TQ. 2015. Bias correction of GCM precipitation by quantile mapping: how well do methods preserve changes in quantiles and extremes? *Journal of Climate* 28: 6938–6959.

Castanho ADA, Galbraith D, Zhang K, Coe MT, Costa MH, Moorcroft P. 2016. Changing Amazon biomass and the role of atmospheric CO_2 concentration, climate and land use. *Global Biogeochemical Cycles* 30: 18–39.

Cernusak LA, Winter K, Dalling JW, Holtum JAM, Jaramillo C, Körner C, Leakey ADB, Norby RJ, Poulter B, Wright SJ. 2013. Tropical forest responses to increasing atmospheric CO_2: current knowledge and opportunities for future research. *Functional Plant Biology* 40: 531–551.

Chen M, Xie P, Janowiak JE, Arkin PA. 2002. Global land precipitation: a 50-yr monthly analysis based on gauge observations. *Journal of Hydrometeorology* 3: 249–266.

Clark DA, Clark DB, Oberbauer SF. 2013. Field-quantified responses of tropical rainforest aboveground productivity to increasing CO_2 and climatic stress, 1997–2009. *Journal of Geophysical Research: Biogeosciences* 118: 783–794.

Comita LS, Engelbrecht BMJ. 2014. Drought as a driver of tropical tree species regeneration dynamics and distribution patterns. In: Coomes DA, Burslem DFRP, Simonson WD, eds. *Forests and global change*. Croydon, UK: Cambridge University Press, 261–308.

Cosby BJ, Hornberger GM, Clapp RB, Ginn TR. 1984. A statistical exploration of the relationships of soil moisture characteristics to the physical properties of soils. *Water Resources Research* 20: 682–690.

da Costa ACL, Galbraith D, Almeida S, Portela BTT, da Costa M, Silva Junior JdA, Braga AP, de Gonçalves PHL, de Oliveira AAR, Fisher R et al. 2010. Effect of 7 yr of experimental drought on vegetation dynamics and biomass storage of an eastern Amazonian rainforest. *New Phytologist* 187: 579–591.

Cox PM, Pearson D, Booth BB, Friedlingstein P, Huntingford C, Jones CD, Luke CM. 2013. Sensitivity of tropical carbon to climate change constrained by carbon dioxide variability. *Nature* 494: 341–344.

Davidson EA, de Araújo AC, Artaxo P, Balch JK, Brown IF, Bustamante MMC, Coe MT, DeFries RS, Keller M, Longo M et al. 2012. The Amazon basin in transition. *Nature* 481: 321–328.

Doughty CE, Metcalfe DB, Girardin CAJ, Amezquita FF, Cabrera DG, Huasco WH, Silva-Espejo JE, Araujo-Murakami A, da Costa MC, Rocha W et al. 2015. Drought impact on forest carbon dynamics and fluxes in Amazonia. *Nature* 519: 78–82.

Duffy PB, Brando P, Asner GP, Field CB. 2015. Projections of future meteorological drought and wet periods in the Amazon. *Proceedings of the National Academy of Sciences, USA* 112: 13172–13177.

Epron D, Bosc A, Bonal D, Freycon V. 2006. Spatial variation of soil respiration across a topographic gradient in a tropical rain forest in French Guiana. *Journal of Tropical Ecology* 22: 565–574.

Erfanian A, Wang G, Fomenko L. 2017. Unprecedented drought over tropical South America in 2016: significantly under-predicted by tropical SST. *Scientific Reports* 7: 5811.

Esquivel-Muelbert A, Galbraith D, Dexter KG, Baker TR, Lewis SL, Meir P, Rowland L, da Costa ACL, Nepstad D, Phillips OL. 2017. Biogeographic distributions of neotropical trees reflect their directly measured drought tolerances. *Scientific Reports* 7: 8334.

Evans MR. 2012. Modelling ecological systems in a changing world. *Philosophical Transactions of the Royal Society B* 367: 181–190.

Farrior CE, Rodriguez-Iturbe I, Dybzinski R, Levin SA, Pacala SW. 2015. Decreased water limitation under elevated CO_2 amplifies potential for forest carbon sinks. *Proceedings of the National Academy of Sciences, USA* 112: 7213–7218.

Feldpausch TR, Phillips OL, Brienen RJW, Gloor E, Lloyd J, Lopez-Gonzalez G, Monteagudo-Mendoza A, Malhi Y, Alarcón A, Álvarez Dávila E et al. 2016. Amazon forest response to repeated droughts. *Global Biogeochemical Cycles* 30: 964–982.

Fine PVA, Miller ZJ, Mesones I, Irazuzta S, Appel HM, Stevens MHH, Sääksjärvi I, Schultz JC, Coley PD. 2006. The growth-defense trade-off and habitat specialization by plants in Amazonian forests. *Ecology* 87: S150–S162.

Fisher R, Koven CD, Anderegg WRL, Christoffersen BO, Dietze MC, Farrior CE, Holm JA, Hurtt GC, Knox RG, Lawrence PJ et al. 2018. Vegetation demographics in Earth System Models: a review of progress and priorities. *Global Change Biology* 24: 35–54.

Fisher R, McDowell N, Purves D, Moorcroft P, Sitch S, Cox P, Huntingford C, Meir P, Woodward IF. 2010. Assessing uncertainties in a second-generation dynamic vegetation model caused by ecological scale limitations. *New Phytologist* 187: 666–681.

Fitzjarrald DR, Sakai RK, Moraes OLL, Cosme de Oliveira R, Acevedo OC, Czikowsky MJ, Beldini T. 2008. Spatial and temporal rainfall variability near the Amazon-Tapajós confluence. *Journal of Geophysical Research: Biogeosciences* 113: G00B11.

Folke C, Carpenter S, Walker B, Scheffer M, Elmqvist T, Gunderson L, Holling CS. 2004. Regime shifts, resilience, and biodiversity in ecosystem management. *Annual Reviews of Ecology, Evolution, and Systematics* 35: 557–581.

Fu R, Yin L, Li W, Arias PA, Dickinson RE, Huang L, Chakraborty S, Fernandes K, Liebmann B, Fisher R et al. 2013. Increased dry-season length over southern Amazonia in recent decades and its implication for future climate projection. *Proceedings of the National Academy of Sciences, USA* 110: 18110–18115.

Galbraith D, Levy PE, Sitch S, Huntingford C, Cox P, Williams M, Meir P. 2010. Multiple mechanisms of Amazonian forest biomass losses in three dynamic global vegetation models under climate change. *New Phytologist* 187: 647–665.

Gloor M, Barichivich J, Ziv G, Brienen R, Schöngart J, Peylin P, Ladvocat Cintra BB, Feldpausch T, Phillips O, Baker J. 2015. Recent Amazon climate as background for possible ongoing and future changes of Amazon humid forests. *Global Biogeochemical Cycles* 29: 1384–1399.

Gloor M, Brienen RJW, Galbraith D, Feldpausch TR, Schöngart J, Guyot J-L, Espinoza JC, Lloyd J, Phillips OL. 2013. Intensification of the Amazon hydrological cycle over the last two decades. *Geophysical Research Letters* 40: 1729–1733.

Good P, Jones C, Lowe J, Betts R, Gedney N. 2013. Comparing tropical forest projections from two generations of hadley centre earth system models, HadGEM2-ES and HadCM3LC. *Journal of Climate* 26: 495–511.

Gourlet-Fleury S, Ferry B, Molino JF, Petronelli P, Schmitt L. 2004. Experimental plots: key features. In: Gourlet-Fleury S, Guehl JM, Laroussinie O, eds. *Ecology and management of a neotropical rainforest: lessons drawn from Paracou, a long-term experimental research site in French Guiana.* Paris, France: Elsevier, 3–60.

Guan K, Pan M, Li H, Wolf A, Wu J, Medvigy D, Caylor KK, Sheffield J, Wood EF, Malhi Y et al. 2015. Photosynthetic seasonality of global tropical forests constrained by hydroclimate. *Nature Geoscience* 8: 284–289.

Hirota M, Holmgren M, Van Nes EH, Scheffer M. 2011. Global resilience of tropical forest and savanna to critical transitions. *Science* 334: 232–235.

Huffman GJ, Adler RF, Bolvin DT, Gu G. 2009. Improving the global precipitation record: GPCP version 2.1. *Geophysical Research Letters* 36: L17808.

Huntingford C, Zelazowski P, Galbraith D, Mercado LM, Sitch S, Fisher R, Lomas M, Walker AP, Jones CD, Booth BBB et al. 2013. Simulated resilience of tropical rainforests to CO_2-induced climate change. *Nature Geoscience* 6: 268–273.

Hutyra LR, Munger JW, Nobre CA, Saleska SR, Vieira SA, Wofsy SC. 2005. Climatic variability and vegetation vulnerability in Amazônia. *Geophysical Research Letters* 32: L24721.

Hutyra LR, Munger JW, Saleska SR, Gottlieb E, Daube BC, Dunn AL, Amaral DF, de Camargo PB, Wofsy SC. 2007. Seasonal controls on the exchange of carbon and water in an Amazonian rain forest. *Journal of Geophysical Research: Biogeosciences* 112: G03008.

Intergovernmental Panel on Climate Change. 2014. Barros VR, Field CB, Dokken DJ, Mastrandrea MD, Mach KJ, Bilir TE. 2012. In: Chatterjee M, Ebi KL, Estrada YO, Genova RC et al., eds. 2014. *Climate change 2014: impacts, adaptation, and vulnerability. Part B: regional aspects. Contribution of Working Group II to the Fifth Assessment Report of the Intergovernmental Panel on Climate Change.* Cambridge, UK & New York, NY, USA: Cambridge University Press.

Ivanov VY, Hutyra LR, Wofsy SC, Munger JW, Saleska SR, de Oliveira RC, de Camargo PB. 2012. Root niche separation can explain avoidance of seasonal drought stress and vulnerability of overstory trees to extended drought in a mature Amazonian forest. *Water Resources Research* 48: W12507.

Jiménez EM, Moreno FH, Peñuela MC, Patiño S, Lloyd J. 2009. Fine root dynamics for forests on contrasting soils in the Colombian Amazon. *Biogeosciences* 6: 2809–2827.

Jiménez-Muñoz JC, Mattar C, Barichivich J, Santamaría-Artigas A, Takahashi K, Malhi Y, Sobrino JA, van der Schrier G. 2016. Record-breaking warming and extreme drought in the Amazon rainforest during the course of El Niño 2015–2016. *Scientific Reports* 6: 33130.

Jirka S, McDonald AJ, Johnson MS, Feldpausch TR, Couto EG, Riha SJ. 2007. Relationships between soil hydrology and forest structure and composition in the southern Brazilian Amazon. *Journal of Vegetation Science* 18: 183–194.

Joetzjer E, Douville H, Delire C, Ciais P. 2013. Present-day and future Amazonian precipitation in global climate models: CMIP5 versus CMIP3. *Climate Dynamics* 41: 2921–2936.

Knox RG. 2012. *Land conversion in Amazonia and Northern South America; influences on regional hydrology and ecosystem response.* PhD thesis, Massachusetts Institute of Technology, Cambridge, MA, USA.

Knox RG, Longo M, Swann ALS, Zhang K, Levine NM, Moorcroft PR, Bras RL. 2015. Hydrometeorological effects of historical land-conversion in an ecosystem-atmosphere model of Northern South America. *Hydrology and Earth System Sciences* 19: 241–273.

Lapola DM, Oyama MD, Nobre CA. 2009. Exploring the range of climate biome projections for tropical South America: the role of CO_2 fertilization and seasonality. *Global Biogeochemical Cycles* 23: GB3003.

Laurance WF, Fearnside PM, Laurance SG, Delamonica P, Lovejoy TE, de Merona JMR, Chambers JQ, Gascon C. 1999. Relationship between soils and Amazon forest biomass: a landscape-scale study. *Forest Ecology and Management* 118: 127–138.

Leitold V, Morton DC, Longo M, Dos-Santos MN, Keller M, Scaranello M. 2018. El Niño drought increased canopy turnover in Amazon Forests. *New Phytologist* 219: 959–971.

Levine NM, Zhang K, Longo M, Baccini A, Phillips OL, Lewis SL, Alvarez E, de Andrade ACS, Brienen R, Erwin T et al. 2016. Ecosystem heterogeneity determines the resilience of the Amazon to climate change. *Proceedings of the National Academy of Sciences, USA* 113: 793–797.

Lewis SL, Brando PM, Phillips OL, van der Heijden GMF, Nepstad D. 2011. The 2010 Amazon drought. *Science* 331: 554.

Liu Z, Ostrenga D, Teng W, Kempler S. 2012. Tropical rainfall measuring mission (TRMM) precipitation data and services for research and applications. *Bulletin of the American Meteorological Society* 93: 1317–1325.

Longo M. 2014. *Amazon forest response to changes in rainfall regime: results from an individual-based dynamic vegetation model.* PhD thesis, Harvard University, Cambridge, MA, USA.

Malhi Y, Aragão LEOC, Galbraith D, Huntingford C, Fisher R, Zelazowski P, Sitch S, McSweeney C, Meir P. 2009. Exploring the likelihood and mechanism of a climate-change-induced dieback of the Amazon rainforest. *Proceedings of the National Academy of Sciences, USA* 106: 20610–20615.

Malhi Y, Roberts JT, Betts RA, Killeen TJ, Li W, Nobre CA. 2008. Climate change, deforestation, and the fate of the Amazon. *Science* 319: 169–172.

Malhi Y, Wood D, Baker T, Wright J, Phillips O, Cochrane T, Meir P, Chave J, Almeida S, Arroyo L et al. 2006. The regional variation of aboveground live biomass in old-growth Amazonian forests. *Global Change Biology* 12: 1107–1138.

Maréchaux I, Bartlett MK, Sack L, Baraloto C, Engel J, Joetzjer E, Chave J. 2015. Drought tolerance as predicted by leaf water potential at turgor loss point varies strongly across species within an Amazonian forest. *Functional Ecology* 29: 1268–1277.

Marengo J, Nobre C, Sampaio G, Salazar L, Borma L. 2011. Climate change in the Amazon basin: tipping points, changes in extremes, and impacts on natural and human systems. In: Bush M, Flenley J, Gosling W, eds. *Tropical rainforest responses to climatic change.* Berlin, Germany: Springer, 259–283.

Marengo JA, Nobre CA, Tomasella J, Oyama MD, De Oliveira GS, De Oliveira R, Camargo H, Alves LM, Brown IF. 2008. The drought of Amazonia in 2005. *Journal of Climate* 21: 495–516.

Marengo JA, Tomasella J, Soares JWR, Alves LM, Nobre CA. 2012. Extreme climatic events in the Amazon basin. *Theoretical and Applied Climatology* 107: 73–85.

Markewitz D, Devine S, Davidson EA, Brando P, Nepstad DC. 2010. Soil moisture depletion under simulated drought in the Amazon: impacts on deep root uptake. *New Phytologist* 187: 592–607.

Marthews TR, Quesada CA, Galbraith DR, Malhi Y, Mullins CE, Hodnett MG, Dharssi I. 2014. High-resolution hydraulic parameter maps for surface soils in tropical South America. *Geoscientific Model Development* 7: 711–723.

Matsuura K, Willmott CJ. 2012. *Terrestrial precipitation: 1900–2010 gridded monthly time series. version 3.01.* [WWW document] URL http://climate.geog.udel.edu/~climate/. [accessed 31 August 2017].

McDowell NG, Allen CD, Anderson-Teixeira K, Brando P, Brienen R, Chambers J, Christoffersen B, Davies S, Doughty C, Duque A et al. 2018. Drivers and mechanisms of tree mortality in moist tropical forests. *New Phytologist* 219: 851–869.

Medvigy D, Moorcroft PR. 2012. Predicting ecosystem dynamics at regional scales: an evaluation of a terrestrial biosphere model for the forests of northeastern North America. *Philosophical Transactions of the Royal Society B* 367: 222–235.

Medvigy DM, Wofsy SC, Munger JW, Hollinger DY, Moorcroft PR. 2009. Mechanistic scaling of ecosystem function and dynamics in space and time: ecosystem demography model version 2. *Journal of Geophysical Research: Biogeosciences* 114: G01002.

Medvigy D, Wofsy SC, Munger JW, Moorcroft PR. 2010. Responses of terrestrial ecosystems and carbon budgets to current and future environmental variability. *Proceedings of the National Academy of Sciences, USA* 107: 8275–8280.

Meinshausen M, Smith SJ, Calvin K, Daniel JS, Kainuma MLT, Lamarque J-F, Matsumoto K, Montzka SA, Raper SCB, Riahi K et al. 2011. The RCP

greenhouse gas concentrations and their extensions from 1765 to 2300. *Climatic Change* **109**: 213–241.

Meir P, Wood TE, Galbraith DR, Brando PM, da Costa ACL, Rowland L, Ferreira LV. 2015. Threshold responses to soil moisture deficit by trees and soil in tropical rain forests: insights from field experiments. *BioScience* **65**: 882–892.

van der Molen MK, Dolman AJ, Ciais P, Eglin T, Gobron N, Law BE, Meir P, Peters W, Phillips OL, Reichstein M *et al.* 2011. Drought and ecosystem carbon cycling. *Agricultural and Forest Meteorology* **151**: 765–773.

Moorcroft PR. 2003. Recent advances in ecosystem-atmosphere interactions: an ecological perspective. *Proceedings of the Royal Society B* **270**: 1215–1227.

Moorcroft PR, Hurtt GC, Pacala SW. 2001. A method for scaling vegetation dynamics: the Ecosystem Demography model (ED). *Ecological Monographs* **71**: 557–586.

Nemani RR, Keeling CD, Hashimoto H, Jolly WM, Piper SC, Tucker CJ, Myneni RB, Running SW. 2003. Climate-driven increases in global terrestrial net primary production from 1982 to 1999. *Science* **300**: 1560–1563.

Nepstad DC, Tohver IM, Ray D, Moutinho P, Cardinot G. 2007. Mortality of large trees and lianas following experimental drought in an Amazon forest. *Ecology* **88**: 2259–2269.

Nobre CA, Borma LS. 2009. 'Tipping points' for the Amazon forest. *Current Opinion in Environmental Sustainability* **1**: 28–36.

Norby RJ, De Kauwe MG, Domingues TF, Duursma RA, Ellsworth DS, Goll DS, Lapola DM, Luus KA, MacKenzie AR, Medlyn BE *et al.* 2016. Model–data synthesis for the next generation of forest free-air CO_2 enrichment (FACE) experiments. *New Phytologist* **209**: 17–28.

Phillips OL, Aragao LEOC, Lewis SL, Fisher JB, Lloyd J, Lopez-Gonzalez G, Malhi Y, Monteagudo A, Peacock J, Quesada CA *et al.* 2009. Drought sensitivity of the Amazon rainforest. *Science* **323**: 1344–1347.

Phillips OL, van der Heijden G, Lewis SL, López-González G, Aragão LEOC, Lloyd J, Malhi Y, Monteagudo A, Almeida S, Alvarez Dávila E *et al.* 2010. Drought-mortality relationships for tropical forests. *New Phytologist* **187**: 631–646.

Powell TL, Galbraith DR, Christoffersen BO, Harper A, Imbuzeiro HMA, Rowland L, Almeida S, Brando PM, da Costa ACL, Costa MH *et al.* 2013. Confronting model predictions of carbon fluxes with measurements of Amazon forests subjected to experimental drought. *New Phytologist* **200**: 350–365.

Powell TL, Wheeler JK, de Oliveira AAR, da Costa ACL, Saleska SR, Meir P, Moorcroft PR. 2017. Differences in xylem and leaf hydraulic traits explain differences in drought tolerance among mature Amazon rainforest trees. *Global Change Biology* **23**: 4280–4293.

Purves D, Pacala S. 2008. Predictive models of forest dynamics. *Science* **320**: 1452–1453.

Pyle EH, Santoni GW, Nascimento HEM, Hutyra LR, Vieira S, Curran DJ, van Haren J, Saleska SR, Chow VY, Carmago PB *et al.* 2008. Dynamics of carbon, biomass, and structure in two Amazonian forests. *Journal of Geophysical Research: Biogeosciences* **113**: G00B08.

Rammig A, Jupp T, Thonicke K, Tietjen B, Heinke J, Ostberg S, Lucht W, Cramer W, Cox P. 2010. Estimating the risk of Amazonian forest dieback. *New Phytologist* **187**: 694–706.

Reich PB, Walters MB, Ellsworth DS. 1997. From tropics to tundra: global convergence in plant functioning. *Proceedings of the National Academy of Sciences, USA* **94**: 13730–13734.

Restrepo-Coupe N, Da Rocha HR, Christoffersen B, de Araújo AC, Borma LS, Cabral OM, de Camargo PB, da Costa ACL, Fitzjarrald DR, Goulden ML *et al.* 2013. What drives the seasonality of productivity across the Amazon basin? a cross-site analysis of eddy flux tower measurements from the Brasil flux network. *Agricultural and Forest Meteorology* **182–183**: 128–144.

Restrepo-Coupe N, Levine NM, Christoffersen BO, Albert LP, Wu J, Costa MH, Galbraith D, Imbuzeiro H, Martins G, de Araújo AC *et al.* 2017. Do dynamic global vegetation models capture the seasonality of carbon fluxes in the Amazon basin? A data-model intercomparison. *Global Change Biology* **23**: 191–208.

Reyer CP, Leuzinger S, Rammig A, Wolf A, Bartholomeus RP, Bonfante A, de Lorenzi F, Dury M, Gloning P, Abou Jaoudé R *et al.* 2013. A plant's perspective of extremes: terrestrial plant responses to changing climatic variability. *Global Change Biology* **19**: 75–89.

Rice A, Pyle E, Saleska S, Hutyra L, Palace M, Keller M, de Camargo P, Portilho K, Marques D, Wofsy S. 2004. Carbon balance and vegetation dynamics in an old-growth Amazonian forest. *Ecological Applications* **14**: S55–S71.

da Rocha HR, Manzi AO, Cabral OM, Miller SD, Goulden ML, Saleska SR, Coupe NR, Wofsy SC, Borma LS, Artaxo P *et al.* 2009. Patterns of water and heat flux across a biome gradient from tropical forest to savanna in brazil. *Journal of Geophysical Research: Biogeosciences* **114**: G00B12.

Rousseeuw P, Croux C, Todorov V, Ruckstuhl A, Salibian-Barrera M, Verbeke T, Koller M, Maechler M. 2015. robustbase: basic robust statistics. *R package version 0.92-3.* [WWW Document] URL https://cran.r-project.org/web/packages/robustbase/index.html. [accessed 31 August 2017].

Rowland L, da Costa ACL, Galbraith DR, Oliveira RS, Binks OJ, Oliveira AAR, Pullen AM, Doughty CE, Metcalfe DB, Vasconcelos SS *et al.* 2015. Death from drought in tropical forests is triggered by hydraulics not carbon starvation. *Nature* **528**: 119–122.

Saatchi SS, Harris NL, Brown S, Lefsky M, Mitchard ETA, Salas W, Zutta BR, Buermann W, Lewis SL, Hagen S *et al.* 2011. Benchmark map of forest carbon stocks in tropical regions across three continents. *Proceedings of the National Academy of Sciences, USA* **108**: 9899–9904.

Saatchi SS, Houghton RA, Alvalá RCDS, Soares JV, Yu Y. 2007. Distribution of aboveground live biomass in the Amazon basin. *Global Change Biology* **13**: 816–837.

Sakschewski B, von Bloh W, Boit A, Poorter L, Pena-Claros M, Heinke J, Joshi J, Thonicke K. 2016. Resilience of Amazon forests emerges from plant trait diversity. *Nature Climate Change* **6**: 1032–1036.

Salazar LF, Nobre CA. 2010. Climate change and thresholds of biome shifts in Amazonia. *Geophysical Research Letters* **37**: L17706.

Saleska S, Miller S, Matross D, Goulden M, Wofsy S, da Rocha H, de Camargo P, Crill P, Daube B, de Freitas H *et al.* 2003. Carbon in Amazon forests: unexpected seasonal fluxes and disturbance-induced losses. *Science* **302**: 1554–1557.

Saleska SR, da Rocha HR, Kruijt B, Nobre A. 2009. Ecosystem carbon fluxes and Amazonian forest metabolism. In: Keller M, Bustamante M, Gash J, Silva Dias PL, eds. *Amazonia and global change*. Washington, DC, USA: American Geophysical Union, 389–407.

Santiago LS, Goldstein G. 2016. Is photosynthesis nutrient limited in tropical trees? In: Goldstein G, Santiago LS, eds. *Tropical tree physiology: adaptations and responses in a changing environment*. Cham, Switzerland: Springer International, 299–315.

Schneider U, Becker A, Finger P, Meyer-Christoffer A, Ziese M, Rudolf B. 2014. GPCC's new land surface precipitation climatology based on quality-controlled *in situ* data and its role in quantifying the global water cycle. *Theoretical and Applied Climatology* **115**: 15–40.

Schwalm CR, Anderegg WRL, Michalak AM, Fisher JB, Biondi F, Koch G, Litvak M, Ogle K, Shaw JD, Wolf A *et al.* 2017. Global patterns of drought recovery. *Nature* **548**: 202–205.

Senna MCA, Costa MH, Pires GF. 2009. Vegetation–atmosphere–soil nutrient feedbacks in the Amazon for different deforestation scenarios. *Journal of Geophysical Research: Atmospheres* **114**: D04104.

Sheffield J, Goteti G, Wood EF. 2006. Development of a 50-year high-resolution global dataset of meteorological forcings for land surface modeling. *Journal of Climate* **19**: 3088–3111.

Swann ALS, Longo M, Knox RG, Lee E, Moorcroft PR. 2015. Future deforestation in the Amazon and consequences for South American climate. *Agricultural and Forest Meteorology* **214–215**: 12–24.

Taylor KE, Stouffer RJ, Meehl GA. 2012. An overview of CMIP5 and the experiment design. *Bulletin of the American Meteorological Society* **93**: 485–498.

Wu J, Albert LP, Lopes AP, Restrepo-Coupe N, Hayek M, Wiedemann KT, Guan K, Stark SC, Christoffersen B, Prohaska N *et al.* 2016. Leaf development and demography explain photosynthetic seasonality in Amazon evergreen forests. *Science* **351**: 972–976.

Würth MKR, Winter K, Körner C. 1998. *In situ* responses to elevated CO_2 in tropical forest understorey plants. *Functional Ecology* **12**: 886–895.

Xu X, Medvigy D, Powers JS, Becknell JM, Guan K. 2016. Diversity in plant hydraulic traits explains seasonal and inter-annual variations of vegetation dynamics in seasonally dry tropical forests. *New Phytologist* **212**: 80–95.

Yang X, Thornton PE, Ricciuto DM, Hoffman FM. 2016. Phosphorus feedbacks constraining tropical ecosystem responses to changes in atmospheric CO_2 and climate. *Geophysical Research Letters* **43**: 7205–7214.

Yin L, Fu R, Shevliakova E, Dickinson RE. 2013. How well can CMIP5 simulate precipitation and its controlling processes over tropical South America? *Climate Dynamics* **41**: 3127–3143.

Zelazowski P, Malhi Y, Huntingford C, Sitch S, Fisher JB. 2011. Changes in the potential distribution of humid tropical forests on a warmer planet. *Philosophical Transaction of the Royal Society A* **369**: 137–160.

Zhang K, Castanho ADdA, Galbraith DR, Moghim S, Levine N, Bras RL, Coe M, Costa MH, Malhi Y, Longo M *et al.* **2015.** The fate of Amazonian ecosystems over the coming century arising from changes in climate, atmospheric CO_2 and land-use. *Global Change Biology* **21**: 2569–2587.

Zimmermann NE, Yoccoz NG, Edwards TC, Meier ES, Thuiller W, Guisan A, Schmatz DR, Pearman PB. 2009. Climatic extremes improve predictions of spatial patterns of tree species. *Proceedings of the National Academy of Sciences, USA* **106**: 19723–19728.

Supporting Information

Additional Supporting Information may be found online in the Supporting Information section at the end of the article.

Fig. S1 Previously published evaluation of the ED2 model, relevant to this study.

Fig. S2 Monthly mean fluxes estimated from ED2, compared with eddy covariance tower estimates.

Fig. S3 Comparison between ED2 predictions and inventory observations of mortality and growth rates.

Fig. S4 Partial auto-correlation evaluation of observed annual rainfall.

Fig. S5 Statistics of annual rainfall for all gridded datasets used in this study.

Fig. S6 Mean annual rainfall for all sites included in the error analysis of the gridded rainfall datasets.

Fig. S7 Average evapotranspiration predicted by ED2 as a function of soil texture and rainfall scenario.

Fig. S8 Example of time series of biomass and drought length for one realization.

Fig. S9 Average size-structure of basal area as a function of rainfall scenarios for additional soil textures.

Fig. S10 Average PFT-structure of basal area as a function of rainfall scenarios for additional soil textures.

Fig. S11 Size- and PFT-dependent average growth rates for rainfall regime scenarios.

Fig. S12 Size- and PFT-dependent average environmentally determined mortality rates for rainfall regime scenarios.

Fig. S13 Stand-level demographic rates as functions of drought length and maximum water deficit.

Fig. S14 Environmental controls of gross primary productivity as functions of DBH class and rainfall scenario at TNF.

Fig. S15 Evapotranspiration:rainfall ratio as a function of drought length and soil texture.

Fig. S16 Average runoff predicted by ED2 as a function of rainfall scenario.

Fig. S17 Example of ecosystem and soil response to interannual variability of rainfall.

Fig. S18 Demographic rates during extreme droughts predicted by ED2 as functions of time since last severe drought.

Fig. S19 Biomass change under elevated CO_2 as a function of the mean return interval of year-long droughts.

Fig. S20 Response of evapotranspiration predicted by ED2 under early and late 21st century atmospheric CO_2.

Table S1 Summary of parameters and configurations used by all simulations

Table S2 Time span and summary of errors associated with each gridded rainfall dataset used in this study

Table S3 Model simulations from CMIP5 that were used in this study

Notes S1 Description of the study site measurements.

Notes S2 Overview of the ED2 model.

Notes S3 Review of the ED2 model evaluation.

Notes S4 Description of the rainfall regime scenarios.

Notes S5 Description of the soil texture datasets.

Notes S6 Weighting factors for each rainfall dataset.

Notes S7 ED2 source code, input data information and script to generate rainfall regime scenarios.

See also the Commentary on this article by Lapola, **219**: 845–847.